Applied Microbiology and Biotechnology
https://doi.org/10.1007/s00253-018-9189-9

APPLIED GENETICS AND MOLECULAR BIOTECHNOLOGY

Catabolism of the groundwater micropollutant 2,6-dichlorobenzamide beyond 2,6-dichlorobenzoate is plasmid encoded in *Aminobacter* sp. MSH1

Jeroen T'Syen[1] · Bart Raes[1] · Benjamin Horemans[1] · Raffaella Tassoni[1] · Baptiste Leroy[2] · Cédric Lood[3,4] · Vera van Noort[3] · Rob Lavigne[4] · Ruddy Wattiez[2] · Hans-Peter E. Kohler[5] · Dirk Springael[1]

Received: 15 May 2018 / Revised: 19 June 2018 / Accepted: 20 June 2018

Abstract

Aminobacter sp. MSH1 uses the groundwater micropollutant 2,6-dichlorobenzamide (BAM) as sole source of carbon and energy. In the first step, MSH1 converts BAM to 2,6-dichlorobenzoic acid (2,6-DCBA) by means of the BbdA amidase encoded on the IncP-1β plasmid pBAM1. Information about the genes and degradation steps involved in 2,6-DCBA metabolism in MSH1 or any other organism is currently lacking. Here, we show that the genes for 2,6-DCBA degradation in strain MSH1 reside on a second catabolic plasmid in MSH1, designated as pBAM2. The complete sequence of pBAM2 was determined revealing that it is a 53.9 kb *repABC* family plasmid. The 2,6-DCBA catabolic genes on pBAM2 are organized in two main clusters bordered by IS elements and integrase genes and encode putative functions like Rieske mono-/dioxygenase, *meta*-cleavage dioxygenase, and reductive dehalogenases. The putative mono-oxygenase encoded by the *bbdD* gene was shown to convert 2,6-DCBA to 3-hydroxy-2,6-dichlorobenzoate (3-OH-2,6-DCBA). 3-OH-DCBA was degraded by wild-type MSH1 and not by a pBAM2-free MSH1 variant indicating that it is a likely intermediate in the pBAM2-encoded DCBA catabolic pathway. Based on the activity of BbdD and the putative functions of the other catabolic genes on pBAM2, a metabolic pathway for BAM/2,6-DCBA in strain MSH1 was suggested.

Keywords 2,6-Dichlorobenzamide · Catabolic pathway · Plasmid encoded · *Aminobacter* · Drinking water treatment

Introduction

Aminobacter sp. MSH1 and related strains are able to mineralize and use the common groundwater micropollutant 2,6-dichlorobenzamide (BAM) as a growth substrate (Sørensen et al. 2007). BAM is a transformation product of the herbicide dichlobenil that has been widely used for weed control in private and agricultural applications. In contrast to its parent compound, BAM is highly mobile and recalcitrant leading to frequent groundwater contamination (Clausen et al. 2004). In groundwater, the compound is encountered at trace concentrations (ng–μg scale) but often exceeds the threshold concentration of 0.1 μg/l for drinking water and hence forms a problem compound for drinking water production (Benner et al. 2013; Helbling 2015). The use of *Aminobacter* sp. MSH1 in dedicated treatment units in drinking water treatment plants (DWTPs) is considered a promising alternative for current treatment approaches of BAM-contaminated groundwater in drinking water production (Albers et al. 2013). However, the pathway and genes used by strain MSH1 and related strains to

Electronic supplementary material The online version of this article (https://doi.org/10.1007/s00253-018-9189-9) contains supplementary material, which is available to authorized users.

✉ Dirk Springael
dirk.springael@kuleuven.be

[1] Division of Soil and Water Management, KU Leuven, Kasteelpark Arenberg 20, 3001 Leuven, Belgium

[2] Department of Proteomics and Microbiology, Research Institute for Biosciences, University of Mons, Place du Parc 20, 7000 Mons, Belgium

[3] Centre of Microbial and Plant Genetics, Department of Microbial and Molecular Systems, KU Leuven, Kasteelpark Arenberg 21, 3001 Leuven, Belgium

[4] Laboratory of Gene Technology, KU Leuven, Kasteelpark Arenberg 21, 3001 Leuven, Belgium

[5] Department of Environmental Microbiology, Swiss Federal Institute of Aquatic Science and Technology (EAWAG), Überlandstrasse 133, Dübendorf 8600, Switzerland

Published online: 08 July 2018

mineralize BAM are largely unknown. Recently, we reported the identification of BbdA, an amidase encoded on a 40.6-kb IncP-1β plasmid, that is responsible for the first step of BAM metabolism in *Aminobacter* sp. MSH1, i.e., the conversion of BAM to 2,6-dichlorobenzoate (2,6-DCBA) (T'Syen et al. 2015). Strain MSH1 and related BAM metabolic strains are among the few bacterial strains reported to degrade and use 2,6-DCBA as a carbon source. Recently, several actinobacteria (*Arthrobacter*, *Microbacterium*, *Rhodococcus*, *Gordonia*) were reported to grow on 2,6-DCBA (Solyanikova et al. 2015) and Abraham et al. (2005) reported that most of the bacterial isolates growing on PCB can degrade 2,6-DCBA. However, in contrast to other chlorinated benzoates (CBAs), no data exist on the genetics and metabolic pathway of 2,6-DCBA biodegradation. Genes for the metabolism of CBAs have been reported in *Pseudomonas aeruginosa* 142 (2-CBA, 2,4-DCBA, 2,5-DCBA) (Romanov and Hausinger 1994; Tsoi et al. 1999); *P. aeruginosa* strain JB2 (2-CBA, 2,3-DCBA, 2,5-DCBA, 2,3,5-TCBA) (Hickey and Focht 1990; Hickey et al. 2001); *Pseudomonas cepacia* 2CBS (2-CBA) (Haak et al. 1995); *Burkholderia* sp. TH2 (2-CBA) (Suzuki et al. 2001); *Pseudomonas putida* AC858 (3-CBA); *Pseudomonas* sp. B13 (3-CBA) (Chatterjee et al. 1981); *Comamonas testosteroni* BR60 (3-CBA, 3,4-DCBA) (Nakatsu et al. 1995); *Cupriavidus pinatubonensis* JMP134 (3-CBA) (Ghosal et al. 1985); *Burkholderia* sp. NK8 (3-CBA, 4-CBA) (Francisco et al. 2001); *Pseudomonas* sp. CBS3 (4-CBA) (Keil et al. 1981), *Alcaligenes* sp. AL3007 (4-CBA) (Layton et al. 1992); and *Pseudomonas* sp. WR912 (3,5-DCBA) (Hartmann et al. 1979). In those strains, biodegradation of CBAs occurs through at least five different pathways, i.e., the chlorocatechol catabolic pathway, hydrolytic dehalogenation, 1,2-dioxygenation, 4,5-dioxygenation (to chloroprotocatechuate) and via gentisate as an intermediate (Pieper 2005; Vrchotova et al. 2013). This study aims at identifying the genes for 2,6-DCBA biodegradation in *Aminobacter* sp. MSH1 and provides further insight in the BAM metabolic pathway of strain MSH1.

Materials and methods

Bacterial strains, cultivation conditions, and chemicals

Strains *Aminobacter* sp. ASI1 (Simonsen et al. 2006), ASI2 (Simonsen 2010), and MSH1 (culture collection number CIP 110285) (Sørensen et al. 2007) were described before. *Aminobacter* sp. strains were routinely grown at 25 °C on either R2A (Reasoner and Geldreich 1985) or minimal medium MMO (Dejonghe et al. 2003) supplemented with 100 to 200 mg/l BAM. The spontaneous mutants *Aminobacter* sp. M1a100g and M6.100g were derived from GFP-labeled variants of MSH1, i.e., strains M1a and M6, respectively, after growth on non-selective medium. Strain A7.100g was derived in an identical way from a RFP labeled variant of ASI2 (A7). Strain M1a100g is unable to convert BAM to 2,6-DCBA but degrades 2,6-DCBA (T'Syen et al. 2015). M6.100g converts BAM to 2,6-DCBA but does not degrade 2,6-DCBA, and strain A7.100g is neither able to perform conversion of BAM to 2,6-DCBA nor to degrade 2,6-DCBA. Additional spontaneous mutants defective in BAM mineralization of MSH1 (M1, M2 and MSH1.100g) and of ASI2 (ASI2.100g) were derived by cultivating the respective parent strains on the non-selective media R2A or MSN mineral medium (Simonsen et al. 2012) supplemented with 4 g/l glucose. Mutants M1 and M2 do not degrade 2,6-DCBA while MSH1.100g and ASI2.100 neither convert BAM to 2,6-DCBA nor degrade 2,6-DCBA. Strains M27.1, M27.2, M27.4, and M27.14 are variants of MSH1 that carry the mini-transposon Tn*5*-RL27 (Larsen et al. 2002). Mutants M27.2 and M27.4 do not convert BAM to 2,6-DCBA but degrade 2,6-DCBA while M27.1 and M27.14, as the wild type, degrade both BAM and 2,6-DCBA. *Escherichia coli* strains TOP10 (Life Technologies) and BL21(DE3)pLysS were cultivated in lysogeny broth (LB) (Bertani 1951). Solid media were prepared using 15 g/l agar. Medium supplements were added when appropriate at the following concentrations: 0.3 mM 2,6-diaminopimelic acid (DAP) and 10 and 20 μg/ml gentamycin (Gm) for *E. coli* and *Aminobacter* strains, respectively. BAM was purchased from Pestanal, UK. Benzamide, benzoic acid (BA), *ortho*-chlorobenzamide (OBAM), *ortho*-chlorobenzoic acid (OBA), and 2,6-DCBA were purchased from Sigma-Aldrich, Belgium. 3-hydroxy-2,6-dichloro-3-benzoic acid (3-OH-2,6-DCBA) was purchased from SynphaBase AG, Switzerland.

DNA isolation

Genomic or plasmid DNA was isolated from *Aminobacter* cultures as previously described (T'Syen et al. 2015).

PCR analysis

PCR detection of plasmid contigs C1, C2, C3, C4, and C5 was performed using the primer pairs reported in Table S1. The PCRs were performed as 50-μl reactions containing 1.25 U of DreamTaq polymerase in 1× PCR buffer (Thermo Scientific), 200 μM of each dNTP, 0.1 mg/ml BSA, 0.1 μM of each primer and 1 μl of template DNA. PCR reactions consisted of 5-min initial denaturation at 94 °C, 30 cycles of 20 s at 94 °C, 20 s at 50 °C (56 °C for C3 amplification), and 30 s at 72 °C and a final extension for 10 min at 72 °C. PCR products were separated by agarose gel electrophoresis (1.5%) in Tris-acetate/EDTA buffer and visualized using ethidium bromide.

Sequencing and bioinformatics analysis

MSH1 plasmid DNA was sequenced on a Roche 454 GS FLX sequencer and assembled into 115 contigs using Newbler 2.6 (Roche) as reported (T'Syen et al. 2015). Paired end (90 bp reads with 454 bp inserts) and mate paired (90 bp reads with 6000 bp inserts) libraries of genomic DNA of MSH1 were sequenced on Illumina GAIIx platforms (BGI) (total depth of sequencing was 142) and assembled into a draft genome sequence of 219 contigs using SOAPdenovo (Luo et al. 2012) with a *k*-mer of 29 (higher *k*-mer values resulted in loss of plasmid specific sequences). A scaffold corresponding to pBAM2 was obtained from the draft genome assembly and appropriate plasmid contigs assembled from the 454 sequence data. Sequence uncertainties in pBAM2 were resolved by obtaining long reads with nanopore sequencing technology. To this end, the genomic DNA of MSH1 was mechanically sheared using a Covaris gTube to an average fragment length of 8 kb. The library preparation was done using the 1D ligation approach, with native 1D barcoding, and the result was sequenced on a SpotION flowcell (R9.4) using the MinION sequencer (Oxford Nanopore Technology). pBAM2 assembly was performed using Unicycler (Wick et al. 2017), which uses a hybrid approach that combines the short reads from Illumina with the long reads from Nanopore. The genome sequence was automatically annotated by rapid annotation using subsystem technology (RAST) (Overbeek et al. 2014) while the sequence of pBAM2 was manually curated. The genome of *Aminobacter* sp. M6.100g was sequenced (90 bp paired reads with 500 bp inserts) on an Illumina GAIIx sequencer, quality trimmed, and mapped onto the consensus sequence of the MSH1 plasmids assembly using SolexaQA (Cox et al. 2010) and Burrows-Wheeler Aligner (bwa-0.6.2) (Li and Durbin 2010) and inspected manually for missing regions as reported previously for strain M1a100g (T'Syen et al. 2015). The pBAM2 plasmid assembly was analyzed using PHASTER (Arndt et al. 2016) to identify and annotate prophage regions within the plasmid.

Differential proteomic analysis

Strain MSH1 and its mutant M6.100g impaired in 2,6-DCBA degradation were cultivated on agar plates containing MMO mineral medium with glucose (500 mg/l) and BAM (200 mg/l) for 3 days. Colonies were inoculated in MSN medium supplemented with glucose (4 g/l) and BAM (200 mg/l) and grown to an OD_{600} of 0.5. After washing in MMO (15 min, 3400×*g* centrifugation), the MSH1 suspension was used to inoculate test tubes containing 10-ml MMO with either glucose (110 mg/l) or BAM (100 mg/l) at an initial OD_{600} of 0.5 while the M6.100g suspension was used to inoculate test tubes containing 10 ml MMO with BAM (100 mg/l). Five replicates were prepared for each condition. BAM degradation was monitored by ultra-high performance liquid chromatography (UHPLC) and cells were harvested by centrifugation (5 min, 15,000×*g*, 4 °C) after 9 h, i.e., when 50% of the BAM was degraded in the test tubes inoculated with MSH1 and stored at − 80 °C prior to protein extraction. Peptide data were acquired using an Eksigent 2D ultra liquid chromatography apparatus combined with a Triple TOF 5600 System (AB Sciex) as described previously (T'Syen et al. 2015). Proteins were identified using Protein pilot 4.0 and a protein database made with genemark.hmm (Lukashin and Borodovsky 1998) based on the draft genome sequence of MSH1. A false discovery rate (FDR) of 1% was applied at protein level. Identified proteins, excluding modified peptides, were used as a background proteome in skyline 2.5 using the MS1 mode of quantification. In skyline, MS resolution was set to 30,000 and retention time windows to 5 min. Exported quantitative data were processed in Excel using an in-house developed procedure filtering available peptides based on deviation on retention time (< 1 min) and IDotP (< 0.75). Only proteins quantified with at least two peptides were taken into account. Proteins were considered differentially regulated if fold change higher than 1.5 or lower than 0.66 was observed with a *p* value lower than 0.05 (unpaired *t* test).

Cloning of putative 2,6-DCBA catabolic genes

The *bbdA* promoter was previously identified as a constitutive promoter in *Aminobacter* sp. MSH1 (T'Syen et al. 2015) and was amplified from genomic DNA of MSH1 using primers PbbdA_F (5′-AAGCGATTAATTAAGTATTCGCCGTGACCTGGTTTCC-3′) and PbbdA_R (5′-AAGCGAGGTACCCATGAGGGCCTGATACGACTTCAC-3′) as reported (T'Syen et al. 2015). The PCR fragment and vector pRU1097 were digested overnight at 37 °C in *Kpn*I buffer with *Pac*I (10 and 4 U for the PCR fragments and the vector, respectively) and *Kpn*I (5 and 2 U for the PCR fragments and the vector, respectively) and the digests purified by gel extraction using QIAEXII (QIAGEN) according to the manufacturer's instructions. Fifty nanogram vector and 50 ng PCR fragment (1:3 M ratio, final volume 12 μl) were ligated by T4 DNA Ligase (0.2 U) in 1× T4 DNA ligase buffer for 10 min at room temperature and cooled on ice. Five microliters of the ligation mixture was mixed with 50-μl chemically competent TOP10 *E. coli* cells and the mixture was incubated for 30 min on ice. A heat shock of 30 s at 42 °C was applied followed by immediate cooling on ice for 2 min. Two hundred fifty microliter SOC medium preheated at 37 °C was added and cells were grown for 1 h at 37 °C while vigorously shaking. Transformants were selected by overnight growth on LB agar plates containing gentamycin (10 mg/l) and the resulting construct,

pRU1097_P_{bbdA}, was checked by PCR, restriction analysis and Sanger sequencing. Selected ORFs (*bbdC*, *bbdD*, *bbdE*, *bbdF*, *bbdG*, *bbdH*, *bbdI*, and $bbdJ_4$) of pBAM2 were amplified by PCR using pairs of primers that contained appropriate restriction site sequences at their 5′ end. The primer sequences are reported in Table S2. The PCR fragments were purified using the DNA Clean and concentrator kit (Zymo research) according to the manufacturer's instructions. The obtained amplicons except the *bbdH* and $bbdJ_4$ amplicons were digested overnight with *Kpn*I (10 U) and *Sac*I (5 U) in 1× Tango buffer (Fermentas) at 37 °C. The *bbdH* amplicon was digested with *Kpn*I (50 U) in 1× Tango buffer for 90 min at 37 °C and subsequently with *Eco*RI in 2× Tango buffer with *Eco*RI (5 U) for 90 min at 37 °C. The $bbdJ_4$ PCR fragment was digested with *Kpn*I (50 U) in 1× Tango buffer for 90 min at 37 °C and subsequently with *Nde*I in 2× Tango buffer with *Eco*RI (5 U) for 90 min at 37 °C. The vector pRU1097_P_{bbdA} was propagated in *E. coli* TOP10 cells in LB with gentamycin (10 mg/l), isolated using QIAprep Spin Miniprep (QIAGEN) and digested using the same conditions and restriction enzymes as mentioned above for the PCR products. Digested vector and PCR fragments were purified by gel extraction using QIAEX II gel extraction kit (QIAGEN) and ligated using approximately 50 ng of vector and insert (molar ratios vector to insert were between 1:2.5 and 1:5) in a volume of 20 μl using T4 DNA ligase (1 U) in 1× T4 DNA ligase buffer (Fermentas) for 10 min at 22 °C and inactivated for 10 min at 65 °C. One microliter of the ligation reactions was mixed with 33 μl of Mix & Go Competent cells—strain Zymo 5α (Zymo research) and incubated on ice for 15 min. Two hundred microliter SOC prewarmed at 37 °C, was added and cells were grown for 1 h at 37 °C. Transformants were selected on LB agar plates with gentamycin (10 mg/l) and the recombinant plasmids checked by Sanger sequencing of the inserts. The resulting recombinant plasmids (named pRU1097_P_{bbdA}_*bbdC* to pRU1097_P_{bbdA}_$bbdJ_4$) were propagated in their hosts in LB with gentamycin (10 mg/l), isolated using QIAprep Spin Miniprep and electroporated into the DAP auxotrophic *E. coli* BW29427. Electroporants were selected on LB agar plates with DAP (0.3 mM) and gentamycin (10 mg/l). Recombinant *E. coli* BW29427 strains were used to transfer the constructs to MSH1 mutant M6.100g (defective in 2,6-DCBA degradation) by biparental conjugation. To this end, recombinant *E. coli* BW29427 cells were grown in LB supplemented with DAP (0.3 mM) and gentamycin (10 mg/l) at 37 °C until an OD_{600} of around 0.9, washed twice in $MgSO_4$ (10 mM) including centrifugation (5500×*g*, 5 min) and set at a final cell density of around 1.5×10^{10} cell/ml. Strain M6.100g, defective in 2,6-DCBA degradation, was grown in MMO mineral medium supplemented with glucose (500 mg/l) and BAM (200 mg/l) at 25 °C until an OD_{600} of 0.3, washed twice in $MgSO_4$ (10 mM) by centrifugation (5500×*g*, 5 min), and resuspended to a final cell density of around 2.50×10^{10} cells/ml. Twenty microliters of the M6.100g suspension and 20 μl of BW29427 containing the pRU1097 constructs were spotted onto sterile Whatman filters and overnight incubated on an R2A agar containing DAP (0.3 mM) at 25 °C. Negative controls consisted of the respective recombinant *E. coli* BW29427 and *Aminobacter* sp. M6.100g strains. After overnight incubation, cells were resuspended, washed twice (5500×*g*, 5 min) in $MgSO_4$ (10 mM), and transconjugants selected on MMO agar containing glucose (500 mg/l) and gentamycin (20 mg/l) at 25 °C. Controls were plated on MMO, MMO with glucose (500 mg/l), and LB with DAP (0.3 mM) agar plates.

2,6-DCBA degradation activity of pBAM2 catabolic genes

M6.100g transconjugants carrying the constructs pRU1097_P_{bbdA}_*bbdC* to pRU1097_P_{bbdA}_$bbdJ_4$ were grown in MMO with glucose (500 mg/l) and gentamycin (20 mg/l) at 25 °C until an OD_{600} of approximately 0.5. Cells were harvested (5500×*g*, 5 min), washed in MMO, and resuspended in MMO supplemented with glucose (500 mg/l) and 2,6-DCBA (200 mg/l) (1.04 mM) at a final cell density of 5.0×10^8 cells/ml. Duplicate cultures were incubated while shaking at 25 °C. Eight hundred microliter samples were taken after 2 and 5 days incubation and immediately inactivated by adding 5 μl HCl (11.65 M). Samples were clarified by centrifugation (21,000×*g*, 10 min) and residual 2,6-DCBA concentration examined by UHPLC analysis. In a separate experiment, the activity of BbdD towards 2,6-DCBA was examined as follows. M6.100g carrying the construct pRU1097_P_{bbdA}_*bbdD* was grown in R2A with gentamycin (20 mg/l), washed (10 min, 5000×*g* centrifugation) and resuspended in MMO to reach a final OD_{600} of 0.5. Cells were harvested (10 min, 5000×*g* centrifugation) and resuspended in either MMO supplemented with 0.45 mM 2,6-DCBA, R2A supplemented with 0.48 mM 2,6-DCBA, or MMO supplemented with 2.78 mM glucose and 0.87 mM 2,6-DCBA, and incubated shaking at 25 °C (one vial per condition). Final cell densities were always 5.0×10^8 cells/ml. Eight hundred-microliter samples were taken and inactivated by adding 5 μl HCl (11.65 M) after 17- and 94-h incubation. After 14 days of incubation, reactivation of 2,6-DCBA degradation was attempted by the addition of nicotinamide adenine dinucleotide (NADH) at a concentration of 3.5 mM (sevenfold molar excess compared to 2,6-DCBA) and continued incubation at 25 °C. Samples were clarified by centrifugation (21,000×*g*, 10 min) before UHPLC analysis.

Identification of the 2,6-DCBA degradation product generated by BbdD

M6.100g carrying recombinant plasmid pRU1097_P_{bbdA}_*bbdD* and M6.100g carrying the vector pRU1097 (used as control)

were precultured in R2A with gentamycin (20 mg/l), washed twice (10 min, 5000×*g* centrifugation) in MMO and resuspended to a final cell density of approximately 1.6×10^{10} cells/ml. Five hundred microliters of the washed cell suspensions were added to MMO containing 2,6-DCBA (200 mg/l) (1.04 mM) and gentamycin (20 mg/l) or MMO with gentamycin (20 mg/l). NADH was added in six doses to the cultures to reach a final concentration of approximately 20 g/l. Abiotic controls with and without NADH supplementation were included in the experimental design. All conditions were prepared in triplicate and were incubated shaking at 25 °C. Eight hundred microliter samples were immediately inactivated with 5 μl HCl (11.65 M), clarified by centrifugation (21,000×*g*, 10 min) and analyzed by UHPLC analysis. The medium was harvested by centrifugation (15 min, 21,000×*g*, 4 °C), frozen and lyophilized for storage. Lyophilized samples were dissolved in 4-ml acidified water (formic acid, pH 2.5) and the metabolite was first purified on a Dionex Summit system with a Dionex P680 pump, a Dionex ASI-100 automated sample injector, and a UVD 340 U photodiode array detector. The compounds were separated on a YMC-Triart C18 column (150 × 3.0 mm, S-3 μm, 12 nm) and detected at 210 nm. The system was operated at a flow rate of 0.400 ml/min with a multistep gradient using eluents A (Nanopure water (Barnstead) acidified to pH 3.1 with formic acid (Sigma-Aldrich)) and C (acetonitrile, Acros Organics). Elution consisted of 3-min isocratic flow using 85% A and 15% C, followed by a 0.5 min linear increase up to 70% A and 30% C and a linear gradient of 6.5 min to a ratio of 40% A and 60% C, which was maintained for 4 min before re-equilibrating the column to the initial eluents composition for 9 min. The results were analyzed and interpreted with Chromeleon software (Dionex, version 6.60). Metabolite purification was performed by manually collecting the eluting metabolite peaks from four injections (250 μl each) and pooling the fractions containing the transformation product. The pooled sample was used to identify the unknown metabolite using reverse-phase liquid chromatography coupled to a high-resolution quadrupole Orbitrap mass spectrometer (Q Exactive, Thermo Scientific). The LC was equipped with a Flux Instruments Rheos 2200 LC/MS pump and was operated with the same column and method as described above for metabolite purification. After each full scan, three data-dependent MS^2 scans in negative ionization mode were conducted. The acquisition was triggered based on assumptions for most probable masses of the metabolite. Full scans and MS^2 were analyzed with XCalibur software (Thermo Scientific, v2.0.7) and compared to spectra of authentic 3-OH-2,6-DCBA.

Degradation of 3-OH-2,6-DCBA by wild type MSH1 and variants M6.100g and M1.100g

Strain MSH1 was cultured in 25 ml of MS with 200 mg/l BAM (1.05 mM) and strains M6.100g and M1.100g in 25 ml of R2A. Cell cultures were harvested (6000×g, 15 min), washed twice in 10 mM $MgSO_4$, and pellets were resuspended in 10 ml of 10 mM $MgSO_4$. Strains MSH1, M1.100g, and M6.100g were inoculated in duplicate in 100-ml Erlenmeyers containing 25 ml of MS medium supplemented with 200 mg/l (0.97 mM) 3-OH-2,6-DCBA at final densities of 2.5×10^8, 10^9, and 10^9 cells/ml, respectively. Cultures were incubated at 25 °C on a shaker (150 rpm). Twice a day, 500-μl samples were taken for determining residual 3-OH-2,6-DCBA concentrations by means of reverse-phase (RP)-UHPLC. None-inoculated Erlenmeyers were included as controls.

RP-UHPLC analysis

Concentrations of BAM, 2,6-DCBA, OBAM, OBA, benzamide, and BA were quantified using RP-UHPLC on a Nexera (Shimadzu Corp) apparatus equipped with a Vision HT C18 HL Column (100 × 2.0 mm, 1.5 μm; Grace, US) and a UV-Vis spectrometer as described (T'Syen et al. 2015). The limits of detection were 41 nM for BAM, 22 nM for 2,6-DCBA, 25 nM for OBAM, 27 nM for OBA, 22 nM for benzamide, and 222 nM for BA. 3-OH-2,6-DCBA was quantified by RP-UHPLC on a Nexera (Shimadzu Corp) apparatus equipped with a Vision HT C18 HL Column (100 × 2.0 mm, 1.5 μm; Grace) and a UV-Vis spectrometer. Elution consisted of 6.5 min of isocratic flow of 5% acetonitrile + 95% ultrapure water (acidified with H_3PO_4 to pH 2.5). A flow rate of 0.2 ml/min and injection volume of 1 μl was used. Detection of the compound was at 210 nm and its retention time was 4.7 min.

Genbank accession number

The nucleotide sequence of plasmid pBAM2 was deposited in Genbank under accession number CP026267.

Results

2,6-DCBA catabolism in *Aminobacter* sp. MSH1 is plasmid encoded

Catabolism of organic xenobiotics is often plasmid encoded (Top et al. 2002). Therefore, the plasmid profile of wild-type strain MSH1 was compared to those of two spontaneous mutants of MSH1 that were able to degrade BAM but unable to degrade 2,6-DCBA, i.e., mutants M1 and M2. Both mutants showed a plasmid profile identical to this of the wild-type MSH1 except for one plasmid that was missing (Fig. 1) indicating that 2,6-DCBA metabolism might be at least partially plasmid encoded in MSH1. To identify the corresponding plasmid, the draft plasmidome of strain MSH1 obtained by 454 sequencing and previously used to compose pBAM1 encoding *bbdA* (T'Syen et al. 2015) was analyzed for other plasmid sequences and catabolic genes. The draft plasmidome consisted

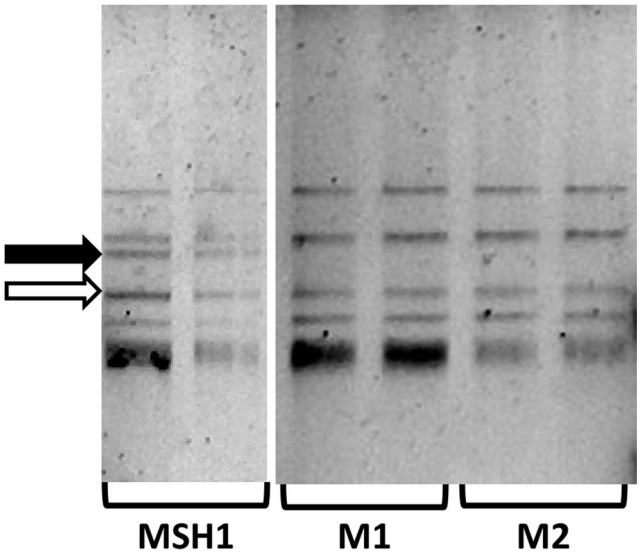

Fig. 1 Plasmid profiles of *Aminobacter* sp. MSH1 and its spontaneous mutants M1 and M2 able to convert BAM to 2,6-DCBA but defective in BAM mineralization and 2,6-DCBA conversion. The black arrow indicates the position of the plasmid in MSH1 that is lacking in mutants M1 and M2. The white arrow indicates plasmid pBAM1 that was previously shown to carry *bbdA* responsible for conversion of BAM into 2,6-DCBA. The lowest band corresponds to fragmented genomic DNA and other bands to other putative plasmids

of 114 unique contigs with a total length of 378 kb. The five largest contigs (93.5, 60.4, 40.4, 28.8, and 27.9 kb) were named C1 to C5, respectively, and revealed backbones of at least five large plasmids, while all other contigs were 5 kb or less. The C3 contig was previously identified as a part of the backbone of IncP-1β plasmid pBAM1 (T'Syen et al. 2015). Annotation and homology-based searches for genes previously associated with CBA degradation within the MSH1 plasmid contigs as well as the complete draft genome of MSH1 using rapid annotation using subsystem technology (RAST) or basic local alignment search tool (BLAST) did not result into significant matches to expected protein functions although several ORFs that could be related to catabolic genes were identified. Therefore, the whole genome of another 2,6-DCBA degradation deficient mutant M6.100g was sequenced by Illumina sequencing. The reads were aligned to the plasmid contigs of strain MSH1 and inspected manually for missing regions. Regions which were entirely missing in mutant M6.100g were the large plasmid contig C4 and five other small contigs, i.e., contigs C6 (4.9 kb), C7 (4.0 kb), C10 (3.1 kb), C11 (2.9 kb), and C13 (2.5 kb). Interestingly, several genes on these contigs were annotated as catabolic genes determining putative functions as catechol 2,3-dioxygenase, maleylacetoacetate isomerase, hydrolase, and vanillate O-demethylase oxygenase. To provide further evidence that those contigs and genes were associated with 2,6-DCBA degradation, the presence of molecular markers associated with them was assessed by PCR in various spontaneous MSH1 mutants (i) deficient in conversion of BAM into 2,6-DCBA but able to degrade 2,6-DCBA, (ii) able to convert BAM into 2,6-DCBA but unable to degrade 2,6-DCBA, or (iii) deficient in both BAM conversion to 2,6-DCBA and degradation of 2,6-DCBA (Fig. S1). The presence of the other plasmid backbone contigs C1, C2, C3, and C5 was assessed as well (Table 1). The loss of 2,6-DCBA degradation was associated with the loss of the genetic marker *trbF* present on plasmid backbone contig C4 while none of the other large plasmid backbones could be related to catabolic phenotypes except C3 associated with pBAM1 and conversion of BAM

Table 1 Results of PCR analysis targeting seven plasmid contigs (C1, C2, C3, C4, C5, C6, and C11) on genomic DNA of *Aminobacter* sp. strains MSH1 and AIS2 and mutants deficient in BAM converion to DCBA and/or further DCBA degradation. BAM and 2,6-DCBA catabolic capabilities of the tested strains are shown

Tested strain*	Catabolic phenotype**		Contig specific PCR signal***						
	Conversion of BAM to 2,6-DCBA	2,6-DCBA conversion	C1	C2	C3	C4	C5	C6	C11
MSH1	+	+	+	+	+	+	+	+	+
MSH1.100g	–	–	+	+	–	–	+	–	–
M1a	+	+	+	+	+	+	+	+	+
M1a.100g	–	+	+	+	–	+	+	+	+
M6	+	+	+	+	+	+	+	+	+
M6.100g	+	–	+	+	+	–	+	–	–
M27.1	+	+	+	+	+	+	+	+	+
M27.2	–	+	+	+	–	+	+	+	+
M27.4	–	+	+	+	–	+	+	+	+
M27.14	+	+	+	+	+	+	+	+	+
M1	+	–	+	+	+	–	+	–	–
ASI2	+	+	+	+	+	+	+	+	+
ASI2.100g	–	–	+	+	–	–	+	–	–
A7	+	+	+	+	+	+	+	+	+
A7.100g	–	–	+	+	–	–	+	–	–

*Strains starting with the letter M are variants of strain MSH1, strains starting with an A are variants of strain ASI2

**+ = the compound is degraded, − = the compound is not degraded

***+ = PCR signal, − = no PCR signal

to 2,6-DCBA (Table 1). Moreover, the presence of genes encoding the vanillate O-demethylase oxygenase homolog (present on plasmid contig C11) and the catechol 2,3-dioxygenase homolog (present on plasmid contig C6) clearly correlated with the capability to degrade 2,6-DCBA, suggesting the involvement of those genes in 2,6-DCBA degradation in strain MSH1 and their physical connection with contig C4.

Sequence of plasmid pBAM2

Efforts were made to completely determine the sequence of the putative 2,6-DCBA catabolic plasmid which was designated as pBAM2. A draft sequence of pBAM2 was assembled by combining sequences obtained from paired (500 bp insert length) and mate paired (8000 bp insert length) whole MSH1 genome Illumina sequencing data and verified using data from the MSH1 draft plasmidome sequence obtained by 454 sequencing. Gaps in the sequences as well as sequence uncertainties related to the presence of identical repeats were solved by long read sequencing using the MinION platform which resulted into a circular scaffold of 53.9 kb. The complete sequence of the plasmid was after automatic annotation was manually curated.

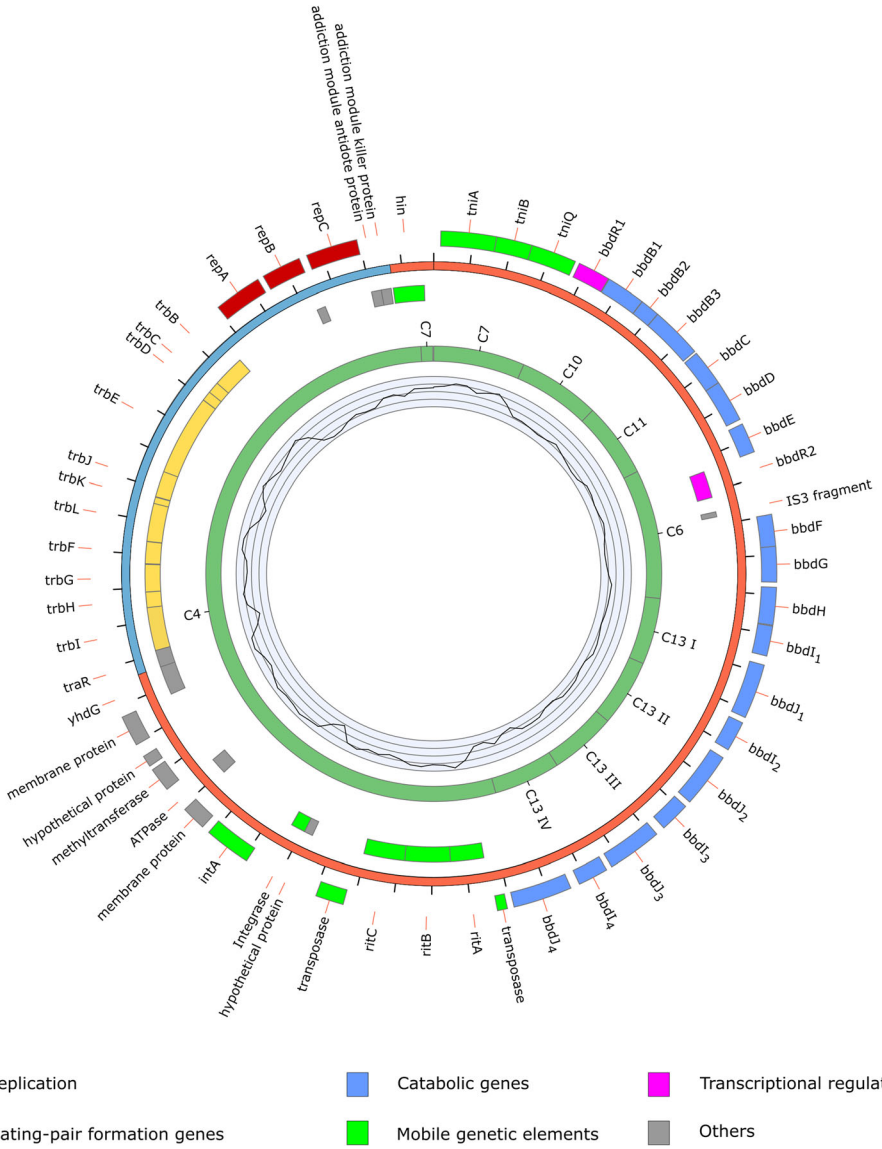

Fig. 2 Circular representation of pBAM2 in *Aminobacter* sp. MSH1 with its annotated putative gene functions indicated on the sense (+) strand (outer circle) and antisense (−) strand (third inward circle). Functional categories are indicated below. The second circle shows the backbone region (red) and the accessory region including the catabolic genes (blue) with ticks indicating 1000-bp intervals. A GC plot is indicated on the most inner circle (from 50 to 70% GC, average GC content is 58%). The green inner circle indicates contigs C4, C6, C7, C10, C11, and C13 assembled from 454 reads onto the hybrid (Illumina and Nanopore) assembly. The C13 contig is only 2.5 kb but maps four times as indicated with I, II, III, and IV

This revealed that plasmid pBAM2 contains in addition to plasmid backbone genes, one large region of catabolic genes that are likely involved in 2,6-DCBA biodegradation (Fig. 2). The region consists of two major gene clusters under different transcriptional control. The putative catabolic genes were designated as *bbd* genes in analogy with *bbdA* encoding BbdA responsible for conversion of BAM to 2,6-DCBA. The first gene cluster *bbdR1B1B2B3CDE*, contains seven ORFs with as predicted gene functions a transcriptional regulator *(bbdR1)*, three subunits of a TRAP-type transport system (*bbdB1*, *bbdB2*, *bbdB3*), a hydrolase (*bbdC*), a mono- or dioxygenase (*bbdD*), and a glutathione S-transferase (*bbdE*). The second gene cluster *bbdFGHIJ* includes ORFs that putatively encode a lactoylglutathione lyase or catechol 2,3-dioxygenase (*bbdF*), a 2-keto-4-pentenoate hydratase/2-oxohepta-3-ene-1,7-dioic acid hydratase or 5-carboxymethyl-2-hydroxymuconate isomerase (*bbdG*), a VanB family oxidoreductase/oxygenase (*bbdH*), a maleylacetoacetate isomerase or glutathione S-transferase (*bbdI*), and a glutathione reductase (*bbdJ*). This gene cluster is immediately followed by three additional copies of the *bbdIJ* gene regions. All four *bbdIJ* regions are identical in sequence except for the most distant in which the *bbdJ* gene is 123 bp longer. We designated the *bbdI* and *bbdJ* copies on pBAM2 as $bbdI_1$ to $bbdI_4$ and $bbdJ_1$ to $bbdJ_4$. A second putative regulatory gene (designated as *bbdR2*) is located in front of the second gene cluster but is transcribed in opposite direction. The catabolic region is separated from the plasmid backbone at both sites by putative transposase and integrase genes. Encoded adjacent to the *bbdR1B1B2B3CDE* catabolic region are proteins showing substantial homology to a phage DNA invertase and three proteins associated with transposons, i.e., TniA (transposase), TniB (NTP-binding protein), and TniQ (transposon-related protein). Adjacent to the *bbdIJ* repeats is a prophage region (80% identity) composed of ORFs encoding three transposases, four integrases, and a hypothetical protein. Two transposases are related to this of IS*1111* elements (IS*110* family) while one is an IS*2* family transposase. The three adjacent putative integrases are encoded on a DNA fragment of 3938 bp that has 87% nucleotide sequence identity to a fragment of the genome of *Novosphingobium* sp. PP1Y bordered by a 61 bp large inverted repeat at both ends. Located between the *bbdR2* and *bbdF* is a remnant of an IS*3* family transposase gene (group IS*51*). A GC plot of pBAM2 (Fig. 2) shows that the catabolic region has a lower average GC content (52.45%) in comparison with the largest part of the backbone region (average GC content 58.24%) except for the *repABC* operon that also shows around 52% GC content.

The presence of the *repABC* operon categorizes pBAM2 as a *repABC* family plasmid commonly found in α-proteobacteria (Petersen et al. 2009). This plasmid family combines all elements needed for replication and partitioning within the *repABC* operon including the RepB binding site *parS* (centromere-like palindrome recognition sequence) and a regulatory counter-transcribed RNA (ctRNA). Two sequences that fit the consensus sequence for *parS* (GTTNNNNGCNNNNAAC) (Cevallos et al. 2008) can be recognized in the *repABC* region of plasmid pBAM2 as well as a sequence that only differs in three positions from the consensus ctRNA promoter sequence (TTGACTGTGATTCGTGGAAGTGCGATTCT (−10 and −35 boxes underlined)) (Cevallos et al. 2008). Phylogenetic analysis of the proteins encoded by the *repABC* operon of plasmid pBAM2 shows that RepA, RepB and RepC have their closest homologs in either *Martelella mediterranea* or *Nitratireductor aquibiodomus* (Fig. 3).

Proteomic study of 2,6-DCBA biodegradation in strain MSH1

To further examine the involvement of plasmid pBAM2 and the *bbdB1B2B3CDE* and *bbdFGHIJ* gene clusters in 2,6-DCBA biodegradation in strain MSH1, a differential proteomic experiment was performed to identify proteins showing an altered abundance in MSH1 after growth on BAM (that is degraded through 2,6-DCBA) on the one hand and growth on equimolar amounts of glucose on the other hand. In addition, the proteome of mutant M6.100g impaired in 2,6-DCBA degradation was compared to this of MSH1 after growing both in MSN medium containing glucose and BAM and a subsequent 9-h incubation in MMO medium containing BAM. Comparison of the proteome of M6.100g to this of MSH1 showed that the majority of the corresponding proteins encoded by pBAM2 where underrepresented or absent in M6.100g. When comparing the proteome of MSH1 cells grown on BAM against this of MSH1 cells grown on glucose, 43 of the 2211 quantified proteins showed an increased abundance (fold change > 1.5; $p < 0.05$) and 94 proteins showed a decreased abundance (fold change < 0.66; $p < 0.05$) (Table 2). Interestingly, four of the catabolic proteins associated with the *bbdFGHIJ* catabolic gene cluster of pBAM2, i.e., *bbdF*, *bbdG*, *bbdH*, and *bbdI* showed an upregulation at protein abundance level when MSH1 was grown on BAM compared to glucose (Table 3) suggesting BAM-dependent expression of these genes. Genes belonging to the *bbdB1B2B3CDE* appeared constitutively expressed (Table 3).

Identification and characterization of the 2,6-DCBA catabolic gene *bbdD*

ORFs of pBAM2 putatively involved in 2,6-DCBA catabolism were selected (*bbdC*, *bbdD*, *bbdE*, *bbdF*, *bbdG*, *bbdH*, *bbdI*, and $bbdJ_4$) and cloned into a broad host range vector derived from the promoter probe vector pRU1097 (Karunakaran et al. 2005). pRU1097 was modified by deletion of the promoterless *gfp-mut3.1* gene and replacing it with the promoter region of *bbdA* (P_{bbdA}) that is constitutively expressed in strain MSH1 (T'Syen et al. 2015). The pBAM2 catabolic ORFs were cloned directly downstream of P_{bbdA}. All

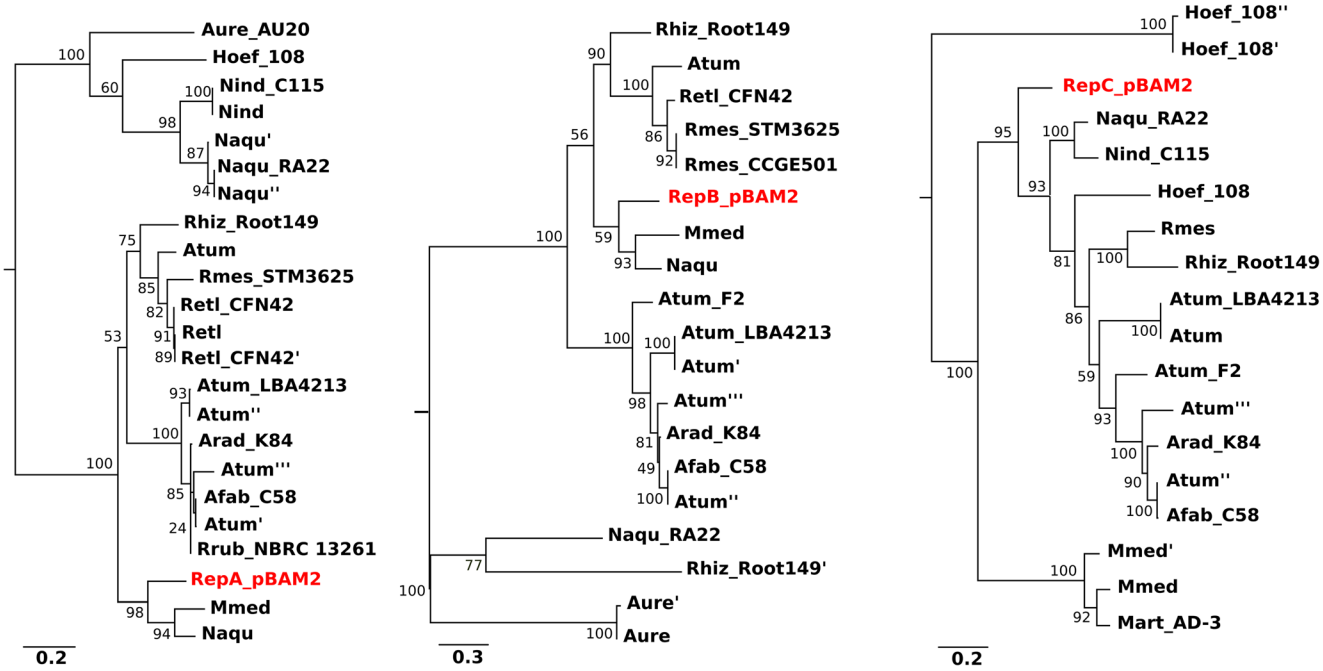

Fig. 3 Phylogenetic trees of pBAM2 RepA, RepB and RepC proteins. Maximum likehood trees created from a clustal-omega (Sievers and Higgins 2014) multiple sequence alignment using selected homologous proteins identified in eight other *α-proteobacterial* taxa (*Aurantimonadaceae*, *Agrobacterium tumefaciens*, *Rhizobium etli*, *Rhizobium mesoamericanum*, *Nitratireductor aquibiodomus*, *Rhizobium* sp. Root149, *Hoeflea* sp. 108, *Martelella* sp. AD-3). The tree was inferred using PhyML (Guindon et al. 2005) with a GTR substitution model and a calculation of branch support values (bootstrap value of 1000). The hosts and accession numbers of selected RepA proteins homologous to pBAM2 RepA are Mmed (*Martelella mediterranea*, WP_026173912.1); Atum (*Agrobacterium tumefaciens*, WP_035227181.1); Retl_CFN42 (*Rhizobium etli* CFN 42, ABC93042.1); Retl_CFN42′ (*Rhizobium etli* CFN 42, AAO43559.1); Retl (*Rhizobium etli*, AAM88937.1); Rhiz_Root149 (*Rhizobium* sp. Root149, KQZ46701.1); Rmes_STM3625 (*Rhizobium mesoamericanum* STM3625, CCM80087.1); Naqu (*Nitratireductor aquibiodomus*, WP_036540573.1); Atum_F2 (*Agrobacterium tumefaciens* F2 EGP53956.1); Rrub_NBRC 13261 (*Rhizobium rubi* NBRC 13261, GAK72154.1); Afab_C58 (*Agrobacterium fabrum* str. C58, AAK91001.2); Arad_K84 (*Agrobacterium radiobacter* K84, ACM31040.1); Atum_LBA4213 (*Agrobacterium tumefaciens* LBA4213 (Ach5), AHK05247.1); Atum′ (*Agrobacterium tumefaciens,* KJX85325.1), Atum″ (*Agrobacterium tumefaciens,* AKC10975.1), Atum‴ (*Agrobacterium tumefaciens* AAZ50477.1); Nind (*Nitratireductor indicus*, WP_040672144.1); Nind_C115 (*Nitratireductor indicus* C115, EKF43267.1); Hoef_108 (*Hoeflea* sp. 108, WP_026227816.1); Naqu′ (*Nitratireductor aquibiodomus*, WP_051556241.1); Naqu_RA22 (*Nitratireductor aquibiodomus* R22, EIM77523.1); Naqu″ (*Nitratireductor aquibiodomus*, WP_052017324.1), Aure_AU20 (*Aureimonas* sp. AU20, ALN74516.1). The hosts and accession numbers of the selected RepB proteins homologous to pBAM2 RepB are Naqu (*Nitratireductor aquibiodomus*, WP_025030991.1); Mmed (*Martelella mediterranea*, WP_018067302.1); Rhiz_Root149 (*Rhizobium* sp. Root149, KQZ46742.1), Rmes_STM3625 (*Rhizobium mesoamericanum* STM3625, CCM80086.1); Rmes_CCGE501 (*Rhizobium mesoamericanum* CCGE 501, AHH29569.1); Retl_CFN42 (*Rhizobium etli* CFN 42, ABC93043.1); Atum (*Agrobacterium tumefaciens*, CDN95698.1); Arad_K84 (*Agrobacterium radiobacter* K84, ACM31041.1); Atum_LBA4213 (*Agrobacterium tumefaciens* LBA4213 (Ach5), AHK05248.1); Atum′ (*Agrobacterium tumefaciens*, WP_040132353.1); Atum_F2 (*Agrobacterium tumefaciens* F2, EGP53955.1); Atum″ (*Agrobacterium tumefaciens*, WP_010891621.1); Afab_C58 (*Agrobacterium fabrum* str. C58, AAF00013.1); Atum‴ (*Agrobacterium tumefaciens*, AAZ50478.1); Aure (*Aureimonas ureilytica*, KTR03976.1); Aure′ (*Aureimonas ureilytica*, KTQ97410.1); Naqu_RA22 (*Nitratireductor aquibiodomus* R22, EIM77524.1); and Rhiz_Root149′ (*Rhizobium* sp. Root149, KQZ62199.1). The hosts and accession numbers of selected RepC proteins homologous to pBAM2 RepC are Naqu_RA22 (*Nitratireductor aquibiodomus* R22, EIM72753.1); Nind_C115 (*Nitratireductor indicus* C115, EKF40256.1), Hoef_108 (*Hoeflea* sp. 108, WP_018431400.1); Atum_F2 (*Agrobacterium tumefaciens* F2, EGP53954.1), Atum (*Agrobacterium tumefaciens*, AKC10977.1); Atum″ (*Agrobacterium tumefaciens*, WP_010891620.1); Arad_K84 (ACM31042.1); Afab_C58 (*Agrobacterium fabrum* str. C58, YP_009076072.1); Rmes (WP_028748912.1); Atum‴ (*Agrobacterium tumefaciens*, YP_001967492.1); Mmed (WP_018067137.1); Atum_LBA4213 (*Agrobacterium tumefaciens* LBA4213 (Ach5), AHK05249.1); Rhiz_Root149 (*Rhizobium* sp. Root149, KQZ46700.1); Mmed′ (*Martelella mediterranea*, WP_026173911.1); Mart_AD-3 (*Martelella* sp. AD-3, WP_024706736.1); Hoef_108′ (*Hoeflea* sp. 108, WP_018431214.1); Hoef_108″ (*Hoeflea* sp. 108, WP_018431021.1); and Naqu (*Nitratireductor aquibiodomus,* gi|640,602,501). Phylogenetic neighbor joining trees using the 100 most similar homologs show similar topologies for all three Rep proteins

constructs were transformed into MSH1 mutant M6.100g defective in 2,6-DCBA degradation and 2,6-DCBA degradation assays were performed to assess whether 2,6-DCBA was degraded. The only construct that showed 2,6-DCBA degrading activity in M6.100g was pRU1097_P_{bbdA}_*bbdD*, containing the putative mono- or dioxygenase (data not shown). The disappearance of 2,6-DCBA was accompanied by the appearance of a compound that eluted as a new UPLC peak approximately at 2.4 min and that likely is the product of 2,6-DCBA conversion (Fig. S2).

Table 2 Summary of the number of proteins identified, proteins with increased abundance and pBAM2 encoded proteins with increased abundance, when comparing the proteomes of (1) MSH1 against its 2,6-DCBA degradation impaired mutant (M6.100g), both grown in the presence of BAM and (2) MSH1 grown in the presence of BAM against MSH1 grown on glucose

	Number of proteins		
	Proteins quantified	Increased protein abundance	Increased pBAM2-encoded protein abundance
MSH1 in BAM versus M6.100g in BAM	2208	41	12
MSH1 grown on BAM versus MSH1 grown on glucose	2211	43	4

However, this activity was only temporary and only a fraction of the initial 2,6-DCBA was converted. The extent of 2,6-DCBA degradation by M6.100g (pRU1097_P_{bbdA}_*bbdD*) depended on the presence of an additional carbon and energy source as more 2,6-DCBA was converted in the presence of glucose and R2A (Fig. 4). Cofactors, like NADH, are required for the catalytic activity of oxygenases (Abu-Omar et al. 2005) and cannot be regenerated in the 2,6-DCBA mineralization-deficient mutant M6.100g without the addition of extra carbon sources. BbdD shows strong similarity with vanillate mono-oxygenase (EC 1.14.13.82) and phenylpropionate dioxygenase (EC 1.14.12.19), both enzymes that utilize NADH as a cofactor. Since the use of crude cell extracts did not reveal any activity and although the uptake of NADH has not been reported, the effect of extracellularly added NADH on the paused 2,6-DCBA degradation activity was tested. Addition of NADH indeed reactivated 2,6-DCBA degradation in M6.100g carrying pRU1097_P_{bbdA}_*bbdD* in R2A medium (Fig. 4).

The putative transformation product of 2,6-DCBA produced by M6.100g carrying pRU1097_P_{bbdA}_*bbdD* was purified and analyzed by mass spectrometry for identification. The monoisotopic molecular ion $[M–H]^-$ showed an exact mass of 204.9466 u corresponding to the molecular formula $C_7H_3Cl_2O_3$, which indicates that the compound is a dichlorohydroxybenzoic acid compound. Comparison with authentic 3-OH-2,6-DCBA shows that both have similar chromatographic retention times in LC and have identical full scan mass spectra and MS^2 spectra of the monoisotopic molecular ion $[M–H]^-$ (Fig. S3). Therefore, it was concluded that the 2,6-DCBA metabolite produced by the BbdD complemented strain is 3-OH-2,6-DCBA, suggesting that BbdD is a 2,6-DCBA hydroxylating mono-oxygenase. To confirm that 3-OH-2,6-DCBA fitted into the degradation pathway encoded on pBAM2 in MSH1, MSH1 wild-type, mutant M6.100g able to convert BAM into 2,6-DCBA but unable to degrade 2,6-DCBA, and mutant M1a.100g unable to convert BAM into 2,6-DCBA but able to degrade 2,6-DCBA, were assessed for the degradation of 3-OH-2,6-DCBA. Wild type MSH1 and mutant M1a.100g degraded 3-OH-2,6-DCBA while mutant M6.100g did not (Fig. S4). Specific 3-OH-2,6-DCBA degradation rates in MSH1 and mutant M1a.100g were highly similar, i.e., 3.9×10^{-9} μg/cell/h in MSH1 and 1.85×10^{-9} μg/cell/h in M1a.100g.

Discussion

Aminobacter sp. MSH1 has the rare ability to completely mineralize BAM, but the mineralization pathway and its coding genes are unknown. In this study, we show that strain MSH1 carries, in addition to pBAM1 that encodes the initial transformation step converting BAM into 2,6-DCBA, a second catabolic plasmid, pBAM2, that encodes for the metabolism of 2,6-DCBA. Genes for pesticide residue biodegradation have been reported before to be plasmid encoded (Martinez et al. 2001; Springael et al. 2001). Most pesticide catabolic plasmids are IncP-1 plasmids often identified in β-proteobacteria and occasionally in other proteobacteria-like plasmid pBAM1 in strain MSH1 that is an α-proteobacterium (T'Syen et al. 2015). In α-proteobacteria, most of the xenobiotic catabolic plasmids were identified in sphingomonads (Basta et al. 2004; Nagata et al. 2007; Tabata et al. 2011). Only a few plasmids carrying xenobiotic degradation genes were identified in α-proteobacteria other than sphingomonads including atrazine degradation in *Pseudaminobacter*, *Chelatobacter*, and *Arthrobacter* strains (Topp et al. 2000; Rousseaux et al. 2002) and BAM degradation in *Aminobacter* sp. MSH1. In addition to pBAM1 and pBAM2, MSH1 appears to contain three more plasmids, having a total of approximately 378 kb of plasmid DNA. Our findings leave the BAM catabolic genes of MSH1 dispersed over two catabolic plasmids and hence, MSH1 needs both plasmids to use BAM as a carbon and energy source. This is quite unusual since in most strains that metabolize organic xenobiotics through plasmid encoded pathways, all genes are located on one plasmid. Other examples though exist like in *Sphingomonas* sp. MM-1 in which the genes for hexachlorocyclohexane degradation are distributed over three plasmids (Tabata et al. 2011). The plot of the average GC content of pBAM2 (Fig. 2) show three distinct regions based on GC content, i.e., the *repABC* operon (GC content of 52.4%), the backbone region (GC content of 58.24%), and the catabolic region (GC content of 52.45%). The average GC content of the genome of *Aminobacter* sp. MSH1 is much higher, i.e., 63.1%, suggesting that all three regions found their way into MSH1 by horizontal gene transfer (Lawrence and Ochman 1997; Eisen 2000).

The *repABC* region categorizes pBAM2 as a *repABC* type plasmid which is commonly found in α-proteobacteria and especially within *Rhizobiales* (Castillo-Ramírez et al. 2009). The *repABC* plasmid family includes other catabolic plasmids (Tabata et al. 2016; accession numbers HE616899,

Table 3 Overview of the ORFs identified in the catabolic region of plasmid pBAM2 with their annotations. ORFs that have multiple identical (or partial) copies on the draft sequence of plasmid pBAM2 are only shown once. The ratio of the protein abundances analyzed by differential proteomic analysis of MSH1 in the presence of BAM versus glucose (ratio BAM versus glucose) and of MSH1 compared to its 2,6-DCBA degradation-deficient mutant M6.100g (ratio MSH1 versus M6.100g) are shown. Number of peptides used for quantification and p value are shown between brackets

Name	Size (bp)	Orientation	Predicted function*	Database accession*	Amino acid identity* (%)	Differential proteomics	
						Ratio MSH1 on BAM versus MSH1 on glucose	Ratio MSH1 versus M6.100g
bbdR1	825	+	Transcriptional regulator (IclR family) HTH-type transcriptional regulator KipR	WP_043834344.1 (*Roseomonas aerilata*) P42968 (*Bacillus subtilis*)	45 27	1.03 (18; 0.66)	9.57 (7; 2.8E-05)
bbdB1	993	+	Substrate-binding protein (TRAP transporter) Solute-binding protein	WP_043766611.1 (*Roseivivax isoporae*) Q122C7 (*Polaromonas* sp.)	37 37	0.80 (20; 0.08)	16.60 (6; 1.3E-04)
bbdB2	495	+	Small permease component (TRAP transporter) Ectoine/5-hydroxyectoine TRAP transporter small permease protein	WP_007009264.1 (*Nitratireductor aquibiodomus*) Q5LUA8 (*Ruegeria pomeroyi*)	36 21	N.D.	N.D.
bbdB3	1314	+	Large permease component (TRAP transporter) Sialic acid TRAP transporter permease protein SiaT	WP_035525091.1 (*Hoeflea* sp. BAL378) P44543 (*Haemophilus influenzae*)	55 27	N.D.	N.D.
bbdC	921	+	Alpha/beta hydrolase Haloalkane dehalogenase	WP_051840613.1 (*Streptomyces* sp. NRRL F-5126) P0A3G3 (*Rhodococcus* sp.)	42 33	0.90 (27; 0.11)	21.16 (3; 1.7E-07)
bbdD	1068	+	Aromatic ring-hydroxylating dioxygenase subunit alpha Toluene-4-sulfonate mono-oxygenase system	WP_017524948.1 (*Pusillimonas noertemannii*) P94679 (*Comamonas testosteroni*)	37 31		
bbdE	762	+	Glutathione S-transferase Tetrachloro-P-hydroquinone reductive dehalogenase	WP_013540554.1 (*Variovorax paradoxus*) Q03520 (*Sphingobium chlorophenolicum*)	39 27	0.92 (17; 0.31)	5.51 (4; 5E-09)
bbdR2	735	–	Transcriptional regulator (IclR family) HTH-type transcriptional regulator KipR	WP_024099485.1 (*Phaeobacter gallaeciensis*) P42968 (*Bacillus subtilis*)	45 22	1.26 (7; 0.05)	6.77 (1; 7.6E-06)
bbdF	867	+	Lactoylglutathione lyase Iron-dependent extradiol dioxygenase	WP_024099484.1 (*Phaeobacter gallaeciensis*) P96850 (*Mycobacterium tuberculosis*)	60 26	8.99 (12; 2.5E-19)	24.77 (5; 6.2E-10)
bbdG	786	+	Fumarylacetoacetate hydrolase Ureidoglycolate lyase	WP_025418322.1 (*Rhizobium leguminosarum*) Q39BA7 (*Burkholderia lata*)	65 38	5.40 (10; 1.9E-05)	3.91 (4; 4.5E-05)
bbdH	957	+	Oxidoreductase N.A.	WP_012079528.1 (*Janthinobacterium* sp. Marseille) N.A.	57 NA	2.53 (8; 1.1E-05)	3.56 (3; 0.01)
bbdI	768	+	Glutathione S-transferase Stringent starvation protein A homolog	WP_068014301.1 (*Rhodoplanes* sp. *Z2-YC6860*) Q83AY0 (*Coxiella burnetii*)	40 42	1.99 (13; 4E-03)	21.40 (4; 1.2E-06)
bbdJ	1347	+	Glutathione disulfide reductase Glutathione amide reductase	WP_046137990.1 (*Devosia epidermidihirudini*) D0VWY5 (*Marichromatium gracile*)	65 37	N.D.	N.D.

*Results of the annotation: search was performed against both non-redundant protein sequences (NCBI) database (upper line) and database of functionally characterized proteins (UniProt) (lower line)

N.D. not detected

CP000638, CP000631) but the most well-known members are the plant transforming Ti plasmid of *Agrobacterium tumefaciens* (Tabata et al. 1989) and plasmids that encode plant symbiotic root nodulation in *Rhizobium* spp. (García-de los Santos et al. 1996). The *repABC* plasmid family includes multiple incompatibility groups allowing co-existence in the same cell (González et al. 2006; Young et al. 2006). Co-existence of multiple compatible *repABC* replicons is also the

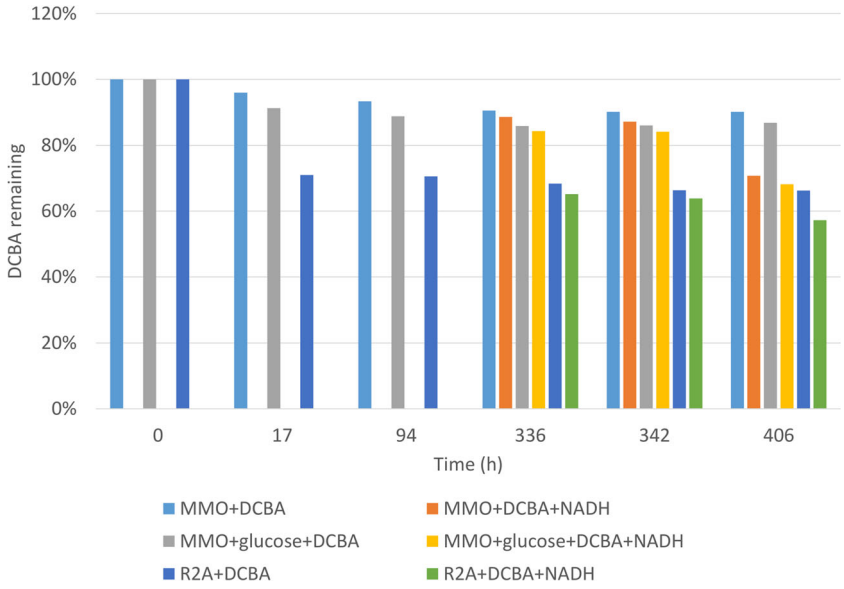

Fig. 4 2,6-DCBA degradation of strain M6.100g carrying pRU1097_P_{bbdA}_*bbdD* as examined in MMO containing 0.45 mM 2,6-DCBA, R2A supplemented with 0.48 mM 2,6-DCBA, or MMO supplemented with 2.78 mM glucose and 0.87 mM 2,6-DCBA. After approximately 14 days (336 h), 2,6-DCBA degradation was reactivated by the addition of NADH (approximately sevenfold molar excess)

case in MSH1 since in addition to pBAM2 another plasmid contig of 93.5 kb (C1) carries a *repABC* operon whose putative RepA, RepB, and RepC proteins show, respectively, 61, 41, and 68% amino acid similarity to those encoded by pBAM2. Horizontal transfer, gene duplication, and divergence and intra-operon recombination are considered as the driving forces of the emergence of new *repABC* plasmid incompatibility groups (Castillo-Ramírez et al. 2009). Crossman et al. (2008) suggest that shuffling of the *repABC* genes is a strategy to allow many plasmids to coexist in the same strain. The conserved region spanning the *trb* genes show most similarity with a fragment of a *repABC* plasmid of *Nitrobacter hamburgensis* X14 (coverage of 88% with 72% identity) (Starkenburg et al. 2008), but also with the *trb* genes of *repABC* plasmid pTiS4 (coverage of 82% with 71% identity) (Slater et al. 2009). The *trb* region in pBAM2 encodes the mating pair formation apparatus required for the physical translocation of DNA from donors to recipients (Li et al. 1999) and is apparently complete to function as such. However, the *tra* region responsible for the effective conjugation step is missing indicating that pBAM2 cannot perform its own transfer.

At the two junctions between the catabolic and backbone regions, i.e., where the shifting of the GC content occurs, genes encoding transposases or remnants of transposases as well as integrases are found suggesting that horizontal gene transfer has also played a role in the acquisition of the catabolic genes by pBAM2. The region containing the integrase shows most similarity with a genome fragment of *Novosphingobium* sp. PP1Y (87% nucleotide identity covering the three integrases and flanking inverted repeats) (D'Argenio et al. 2014). Also plasmid pTiS4 carries a fragment that shows 90% nucleotide identity but covers only half of the integrase region of pBAM2 (Slater et al. 2009). The three integrase genes encode proteins that have C-terminal catalytic domains similar to these of RitA, RitB, and RitC, encoded by a recombinase in trio (RIT) genetic element and are flanked at both ends by IRs, as found for several other RIT elements (Ricker et al. 2013). RIT elements are abundant in α-proteobacteria and are associated with both intragenomic and interspecies mobility of DNA fragments, which in some cases could be linked to plasmid intermediates. Interestingly, 42% of the bacterial isolates carrying RIT elements were isolated from contaminated environments and RIT elements have been reported previously flanking the chlorocatechol degradation genes of the CBA-degrading *Burkholderia phytofirmans* OLGA172 (Jin 2010). A remnant of an IS*3* transposase gene is also present in the middle of the catabolic region. This might be a scar from the recruitment of the catabolic genes which might indicate that the two gene clusters were recruited independently. Otherwise, it might have been introduced after catabolic gene recruitment. For most genes in the catabolic region, no obvious ancestral origin can be deduced based on protein homology (Table 3), since most of the corresponding proteins find their closest relatives in different genera. The exception are proteins BbdR2, BbdF, and BbdG which have their closest annotated homologs encoded in the same order and orientation on plasmid pGal_C110 in the marine α-proteobacterium *Phaeobacter gallaeciensis* DSM 26640 (Seyedsayamdost et al. 2011) albeit without the presence of the transposase remnant between the *bbdR2* and *bbdF* homologs. An identical organization of homologous genes is also found in *Rhizobium leguminosarum* bv. Trifolii and in *Labrenzia alba* while in *Agrobacterium vitis* S4 and *M. mediterranea* homologs are found but they are not forming an operon (data not shown). Apart from being recruited, the catabolic gene regions show additional features of evolution, i.e., the region carries four copies of the catabolic genes *bbdIJ*. Repeats of catabolic genes on organic xenobiotic catabolic plasmids were reported previously

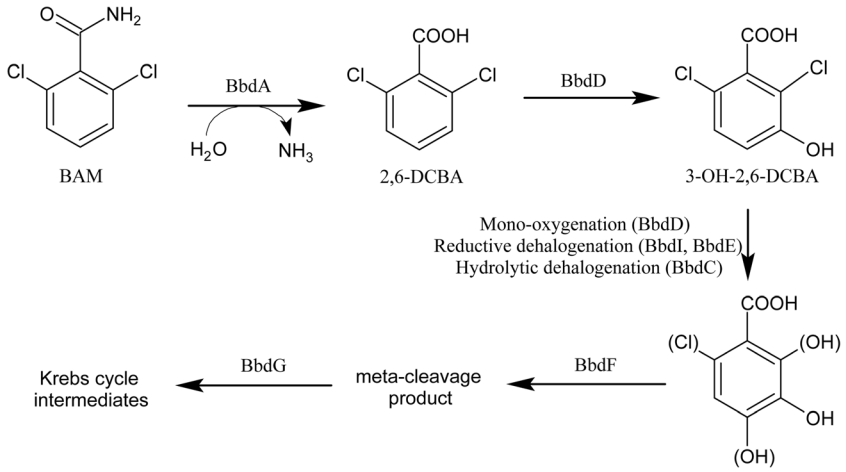

Fig. 5 Putative BAM/2,6-DCBA catabolic pathway in *Aminobacter* sp. MSH1 based on the functions associated with the putative 2,6-DCBA catabolic proteins encoded by pBAM2. BAM is converted to 2,6-DCBA by the amidase BbdA encoded on pBAM1 (T'Syen et al. 2015). The mono-oxygenase BbdD converts 2,6-DCBA to 3-OH-2,6-DCBA which is converted to a (chlorinated) dihydroxylated benzoic acid with a yet unknown isomeric structure potentially involving BbdD and/or BbdC. Meta-cleavage of the (chlorinated) dihydroxylated benzoic acid by BbdF results in ring opening. BbdG (lyase) is potentially involved in further conversion of the *meta*-cleavage product to Krebs cycle intermediates. BbdE and BbdI are putative glutathione S-transferases and are proposed to be involved in removing one or two chlorines by means of reductive dehalogenation before or after ring cleavage. Aromatic OH and Cl substitutions between brackets indicate positions that are substituted or not. Only one of the two OH substitutions after 3-OH-2,6-DCBA formation is possible. pBAM2 genes indicated between brackets indicate a possible involvement in the reaction step

and often evolve after growing the organism under selective conditions. Gene dosage advantages could be beneficiary for the host for improved growth on the xenobiotic or to overcome metabolic bottlenecks (Pieper et al. 1993; Klemba et al. 2000; Clement et al. 2001). The tandem repeats on pBAM2 might have a similar role in growth on 2,6-DCBA. This region encodes a glutathione S-transferase (*bbdI*) and a glutathione reductase (*bbdJ*) likely involved in chlorine removal.

Complementation experiments showed that BbdD can convert 2,6-DCBA into 3-OH-2,6-DCBA. BbdD shows sequence similarity to proteins with various putative mono- and dioxygenase functions. Most similarity was found with a putative (TsaM2, accession Q9AHG3) and an experimentally confirmed (TsaM1, accession P12609) toluene-4-sulfonate mono-oxygenase (95% coverage with 34 and 31% amino acid identity, respectively) followed by two vanillate O-demethylase oxygenases (VanA) (accession O05616 and accession P12609 showing 29% (86% coverage) and 32% identity (80% coverage), respectively). TsaM1 and TsaM2 are encoded on the IncP-1β plasmid pTSA and catalyze the conversion of *p*-toluenesulfonate to *p*-sulfobenzyl alcohol in *C. testosteroni* T-2 (Locher et al. 1991; Tralau et al. 2001). The vanillate mono-oxygenase VanA converts vanillate to protocatechuate as a step in lignin degradation in several bacteria, including *Pseudomonas* sp. HR199 (Schuler et al. 2009; Riefert et al. 1997) and *Rhodococcus jostii* RHA1 (Chen et al. 2012). BbdD shows several features of mono- and di-oxygenases including a predicted N-terminal Rieske non-heme iron oxygenase family domain with a [2Fe–2S] cluster (accession cd03532) and a C-terminal ligand-binding SRPBCC domain carrying Fe(II) (accession cl14643). Together, these domains form the alpha oxygenase subunit of Rieske-type non-heme iron aromatic ring-hydroxylating oxygenases such as in the homologous VanA and TsaM1. The [2Fe–2S] cluster of such proteins accepts electrons from a reductase or ferredoxin component and transfers these to the iron atom for catalysis (Ferraro et al. 2005). Both TsaM1 and VanA require an iron-sulfur flavoprotein reductase, TsaB and VanB, respectively, to supply electrons from NADH to the oxygenase subunit. The lack of the auxiliary protein in the MSH1 constructs carrying only BbdD likely explains the poor activity of BbbD towards DCBA. Probably, in the construct, this function is at least partially accomplished by host proteins as previously observed (Prieto and Garcia 1994; Bertoni et al. 1998). pBAM2 encodes a VanB homolog, BbdH, which could play that role for BbdD. BbdH shows 48% amino acid identity (95% coverage) to the vanillate O-demethylase oxidoreductase VanB of *Pseudomonas* sp. HR199 (accession O05617). The sequence of BbdH further shows the presence of an N-terminal NADH binding domain (accession cd06185) and a C-terminal iron-sulfur [2Fe–2S] cluster binding domain (accession cd00207). These domains are found in FMN-dependent reductases that mediate electron transfer from NADH to FMN to an iron-sulfur cluster like in TsaB (accession AAC44805) and VanB (accession CAA72288). Several attempts to improve BbdD activity by including BbdH were however unsuccessful (data not shown). The product of 2,6-DCBA conversion was 3-OH-DCBA. 3-OH-DCBA conversion was only observed in case MSH1 carried pBAM2, which strongly suggests that 3-OH-DCBA is a true intermediate in the DCBA catabolic pathway and hence the involvement of BbdD enzyme in the first step of 2,6-DCBA biodegradation in MSH1.

The *meta*-hydroxylation reaction of 2,6-DCBA into 3-OH-DCBA rules out that *Aminobacter* sp. MSH1 uses a BAM catabolic pathway producing 2-chlorobenzoate as an catabolic intermediate (Holtze et al. 2007). Potential pathways for 2,6-DCBA and 3-OH-2,6-DCBA predicted by the EAWAG-BBD Pathway Prediction System (Gao et al. 2011) required protein functions incompatible to the annotated protein functions of the other Bbd proteins. Therefore, an attempt was made to propose a plausible 2,6-DCBA pathway using the annotated protein functions as shown in Fig. 5. The annotations would implicate that BbdH, BbdJ, and BbdK do not catalyze catabolic reactions but rather have supporting functions, like the provision of electrons to BbdD by the FNM-dependent reductase BbdH or the regeneration of glutathione used by BbdE or BbdI by the glutathione reductases BbdJ or BbdK. This leaves five putative proteins involved in further conversion of 3-OH-2,6-DCBA encoded on pBAM2, i.e., BbdC (alpha/beta hydrolase), BbdE (glutathione S-transferase), BbdF (lactoylglutathione lyase or catechol 2,3-dioxygenase), BbdG (2-keto-4-pentenoate hydratase/2-oxohepta-3-ene-1,7-dioic acid hydratase or 5-carboxymethyl-2-hydroxymuconate isomerase) and BbdI (glutathione S-transferase). The putative glutathione S-transferases BbdE and BbdI could have various functions like a β-etherase, isomerase or reductive dehalogenase. The reductive dehalogenase function is of major interest since it indicates the occurrence of chlorine removal steps either before and/or after ring cleavage. Furthermore, the putative catechol 2,3-dioxygenase function of BbdF indicates that *meta*-cleavage of the aromatic ring occurs and that the further degradation of 3-OH-2,6-DCBA proceeds through a dihydroxylated (chloro)benzoic acid derivative with yet unknown structure such as a protocatechuate, gentisate or 2,3-dihydroxybenzoate like compound. Hence, a mono-hydroxylated degradation intermediate (either 3-OH-2,6-DCBA or a dechlorinated variant) needs to be converted into a chlorinated dihydroxylated benzoic acid before it can be degraded by BbdF. This would insinuate a second mono-oxygenase step in the pathway. A second mono-oxygenase gene is however not present in the two pBAM2 catabolic clusters and the hypothesis that this step is performed by a gene encoded elsewhere in the genome is highly unlikely taking into account that 3-OH-2,6-DCBA is not degraded further in a MSH1 mutant lacking pBAM2. This leaves three alternatives: (i) BbdD is also responsible for the second mono-oxygenation step but it was not observed due to the low activity; (ii) BbdD is responsible for the second mono-oxygenation step but does this only after 3-OH-DCBA has been converted, e.g., after a dehalogenation step; or (iii) the second hydroxyl group is added using an alternative enzymatic mechanism. A candidate for the latter is BbdC that shows substantial similarity with alpha/beta hydrolases that hydrolytically dehalogenate aliphatic replacing the chlorine atom by a hydroxyl group originating from water (Koudelakova et al. 2013). The hydroxylation of the chlorine substitution at the *ortho* position adjacent to the hydroxyl group of 3-OH-DCBA would create an aromatic compound with two vicinal hydroxyl groups amenable to *meta*-cleavage. Finally, the BbdG (lyase) protein might be involved in the further conversion of the *meta*-cleavage product in Krebs cycle intermediates like oxaloacetate and pyruvate. In addition to the putative catabolic proteins, pBAM2 also carries a putative tripartite ATP-independent periplasmic (TRAP) transporter encoded by *bbdB1*, *bbdB2*, and *bbdB3*. This family of transporters are mostly involved in the uptake of organic acids and combine a substrate binding protein (putatively BbdB1) with a transporter consisting of a small (putatively BbdB2) and large (putatively BbdB3) permease component (Mulligan et al. 2011). The co-localization of these genes directly upstream of the 2,6-DCBA catabolic genes could be a remnant of the transport of a benzoic acid like compound (co-evolution with adjacent catabolic genes) or could be effectively involved in the uptake of 2,6-DCBA. Indeed, 2,6-DCBA was appointed a bottleneck for BAM mineralization in MSH1 and other BAM-degrading *Aminobacter* strains resulting into accumulation of 2,6-DCBA in the medium and hence has to be retaken by the cells for its further metabolism (Simonsen et al. 2012).

Acknowledgements The authors thank J. Aamand for providing strains MSH1, ASI1, and ASI2; Dianne K. Newman for providing *E. coli* BW29427, A. Provoost for skillful help in plasmid isolation, M. Everaert for lyophilization, T. Fleischmann and I. Schilling for helping with HPLC-MS and identification of 3-OH-2,6-DCBA, and J. Cornelis for technical assistance.

Funding This work was supported by IWT-Vlaanderen Strategic Basic Research project [grant number 101589], the Inter-University Attraction Pole (IUAP) "μ-manager" of the Belgian Science Policy (BELSPO) [grant number P7/25], EU project BIOTREAT [EU grant number 266039] and by the FNRS under grant "grand equipment" [grant number2877824]. CL was supported by an SB PhD fellowship [grant number 1S64718N] and BH by a postdoctoral fellowship [grant number12Q0218N] from FWO Vlaanderen.

Compliance with ethical standards

Conflict of interest The authors declare that they have no competing interests.

Ethical statement This article does not contain any studies with human participants or animals performed by any of the authors.

References

Abraham W-R, Wenderoth DF, Gläßer W (2005) Diversity of biphenyl degraders in a chlorobenzene polluted aquifer. Chemosphere 58(4): 529–533. https://doi.org/10.1016/j.chemosphere.2004.08.074

Abu-Omar M, Loaiza A, Hontzeas N (2005) Reaction mechanisms of mononuclear non-heme iron oxygenases. Chem Rev 105(6):2227–2252

Albers CN, Jacobsen OS, Aamand J (2013) Using 2,6-dichlorobenzamide (BAM) degrading *Aminobacter* sp. MSH1 in flow through biofilters—initial adhesion and BAM degradation

potentials. Appl Microbiol Biotechnol 98(2):957–967. https://doi.org/10.1007/s00253-013-4942-6

Arndt D, Grant JR, Marcu A, Sajed T, Pon A, Liang Y, Wishart DS (2016) PHASTER: a better, faster version of the PHAST phage search tool. Nucleic Acids Res 44(W1):W16–W21. https://doi.org/10.1093/nar/gkw387

Basta T, Keck A, Klein J, Stolz A (2004) Detection and characterization of conjugative degradative plasmids in xenobiotic-segrading *Sphingomonas* strains. J Bacteriol 186(12):3862–3872. https://doi.org/10.1128/JB.186.12.3862-3872.2004

Benner J, Helbling DE, Kohler H-PE, Wittebol J, Kaiser E, Prasse C, Ternes TA, Albers CN, Aamand J, Horemans B, Springael D, Walravens E, Boon N (2013) Is biological treatment a viable alternative for micropollutant removal in drinking water treatment processes? Water Res 47(16):5955–5976. https://doi.org/10.1016/j.watres.2013.07.015

Bertani G (1951) Studies on lysogenesis I.: the mode of phage liberation by lysogenic *Escherichia coli*. J Bacteriol 62(3):293–300

Bertoni G, Martino M, Galli E, Barbieri P (1998) Analysis of the gene cluster encoding toluene/o-xylene monooxygenase from *Pseudomonas stutzeri* OX1. Appl Environ Microbiol 64(10):3626–3632

Castillo-Ramírez S, Vázquez-Castellanos JF, González V, Cevallos MA (2009) Horizontal gene transfer and diverse functional constrains within a common replication-partitioning system in Alphaproteobacteria: the *repABC* operon. BMC Genomics 10:536. https://doi.org/10.1186/1471-2164-10-536

Cevallos MA, Cervantes-Rivera R, Gutiérrez-Ríos RM (2008) The *repABC* plasmid family. Plasmid 60(1):19–37. https://doi.org/10.1016/j.plasmid.2008.03.001

Chatterjee DK, Kellogg ST, Hamada S, Chakrabarty AM (1981) Plasmid specifying total degradation of 3-chlorobenzoate by a modified *ortho* pathway. J Bacteriol 146(2):639–646

Chen H, Chow M, Liu C, Lau A, Liu J, Eltis L (2012) Vanillin catabolism in *Rhodococcus jostii* RHA1. Appl Environ Microbiol 78(2):586–588. https://doi.org/10.1128/AEM.06876-11

Clausen L, Larsen F, Albrechtsen H-J (2004) Sorption of the herbicide dichlobenil and the metabolite 2,6-dichlorobenzamide on soils and aquifer sediments. Environ Sci Technol 38(17):4510–4518. https://doi.org/10.1021/es035263i

Clement P, Pieper D, Gonzalez B (2001) Molecular characterization of a deletion/duplication rearrangement in tfd genes from *Ralstonia eutropha* JMP134(pJP4) that improves growth on 3-chlorobenzoic acid but abolishes growth on 2,4-dichlorophenoxyacetic acid. Microbiology 147:2141–2148. https://doi.org/10.1099/00221287-147-8-2141

Cox M, Peterson D, Biggs P (2010) SolexaQA: at-a-glance quality assessment of Illumina second-generation sequencing data. BMC Bioinformatics 11:485. https://doi.org/10.1186/1471-2105-11-485

Crossman LC, Castillo-Ramírez S, McAnnula C, Lozano L, Vernikos GS, Acosta JL, Ghazoui ZF, Hernández-González I, Meakin G, Walker AW, Hynes MF, Young JPW, Downie JA, Romero D, Johnston AWB, Dávila G, Parkhill J, González V (2008) A common genomic framework for a diverse assembly of plasmids in the symbiotic nitrogen fixing bacteria. PLoS One 3(7):e2567. https://doi.org/10.1371/journal.pone.0002567

D'Argenio V, Notomista E, Petrillo M, Cantiello P, Cafaro V, Izzo V, Naso B, Cozzuto L, Durante L, Troncone L, Paolella G, Salvatore F, Di Donato A (2014) Complete sequencing of *Novosphingobium* sp. PP1Y reveals a biotechnologically meaningful metabolic pattern. BMC Genomics 15:384. https://doi.org/10.1186/1471-2164-15-384

Dejonghe W, Berteloot E, Goris J, Boon N, Crul K, Maertens S, Höfte M, De Vos P, Verstraete W, Top EM (2003) Synergistic degradation of linuron by a bacterial consortium and isolation of a single linuron-degrading *Variovorax* strain. Appl Environ Microbiol 69(3):1532–1541

Eisen JA (2000) Horizontal gene transfer among microbial genomes: new insights from complete genome analysis. Curr Opin Genet Dev 10(6):606–611. https://doi.org/10.1016/S0959-437X(00)00143-X

Ferraro D, Galhar L, Ramaswamy S (2005) Rieske business: structure–function of Rieske non-heme oxygenases. Biochem Biophys Res Commun 338(1):175–190. https://doi.org/10.1016/j.bbrc.2005.08.222

Francisco N, Suzuki K, Miyashita KP, Ogawa (2001) The chlorobenzoate dioxygenase genes of *Burkholderia* sp. strain NK8 involved in the catabolism of chlorobenzoates. Microbiology 147(1):121–133. https://doi.org/10.1099/00221287-147-1-121

Gao J, Ellis L, Wackett L (2011) The University of Minnesota pathway prediction system: multi-level prediction and visualization. Nucleic Acids Res 39:W406–W411. https://doi.org/10.1093/nar/gkr200

García-de los Santos A, Brom S, Romero D (1996) *Rhizobium* plasmids in bacteria-legume interactions. World J Microbiol Biotechnol 12(2):119–125. https://doi.org/10.1007/BF00364676

Ghosal D, You IS, Chatterjee DK, Chakrabarty AM (1985) Genes specifying degradation of 3-chlorobenzoic acid in plasmids pAC27 and pJP4. Proc Natl Acad Sci U S A 82:1638–1642

González V, Santamaría R, Bustos P, Hernández-González I, Medrano-Soto A, Moreno-Hagelsieb G, Janga S, Ramírez M, Jiménez-Jacinto V, Collado-Vides J (2006) The partitioned *Rhizobium etli* genome: genetic and metabolic redundancy in seven interacting replicons. Proc Natl Acad Sci U S A 103(10):3834–3839. https://doi.org/10.1073/pnas.0508502103

Guindon S, Lethiec F, Duroux F, Gaccuel O (2005) PHYML online—a web server for fast maximum likelihood-based phylogenetic inference. Nucleic Acids Res 33(2):W557–W559

Haak B, Fetzner S, Lingens F (1995) Cloning, nucleotide sequence, and expression of the plasmid-encoded genes for the two-component 2-halobenzoate 1,2-dioxygenase from *Pseudomonas cepacia* 2CBS. J Bacteriol 177(3):667–675

Hartmann W, Knackmuss HJ, Reineke J (1979) Metabolism of 3-chloro-, 4-chloro-, and 3,5-dichlorobenzoate by a pseudomonad. Appl Environ Microbiol 37(3):421–428

Helbling DE (2015) Bioremediation of pesticide-contaminated water resources: the challenge of low concentrations. Curr Opin Biotechnol 33:142–148. https://doi.org/10.1016/j.copbio.2015.02.012

Hickey WJ, Focht DD (1990) Degradation of mono-, di-, and trihalogenated benzoic acids by *Pseudomonas aeruginosa* JB2. Appl Environ Microbiol 56(12):3842–3850

Hickey WJ, Sabat G, Yuroff AS, Arment AR, Pérez-Lesher J (2001) Cloning, nucleotide sequencing, and functional analysis of a novel, mobile cluster of biodegradation genes from *Pseudomonas aeruginosa* strain JB2. Appl Environ Microbiol 67(10):4603–4609. https://doi.org/10.1128/AEM.67.10.4603-4609.2001

Holtze MS, Hansen HCB, Juhler RK, Sørensen J, Aamand J (2007) Microbial degradation pathways of the herbicide dichlobenil in soils with different history of dichlobenil-exposure. Environ Pollut 148(1):343–351. https://doi.org/10.1016/j.envpol.2006.10.028

Jin S (2010) Evidence of mobility in the 3-chlorobenzoate degradative genes in a pristine soil isolate, *Burkholderia phytofirmans* OLGA172. University of Toronto, Canada

Karunakaran R, Mauchline TH, Hosie AHF, Poole PS (2005) A family of promoter probe vectors incorporating autofluorescent and chromogenic reporter proteins for studying gene expression in gram-negative bacteria. Microbiology 151(10):3249–3256. https://doi.org/10.1099/mic.0.28311-0

Keil U, Lingens FH, Klages (1981) Degradation of 4-chlorobenzoate by *Pseudomonas* sp. CBS3: Induction of catabolic enzymes. FEMS Microbiol Lett 10(2):213–215. https://doi.org/10.1111/j.1574-6968.1981.tb06240.x

Klemba M, Jakobs B, Wittich R-M, Pieper D (2000) Chromosomal integration of *tcb* chlorocatechol degradation pathway genes as a means of expanding the growth substrate range of bacteria to include

haloaromatics. Appl Environ Microbiol 66(8):3255–3261. https://doi.org/10.1128/AEM.66.8.3255-3261.2000

Koudelakova T, Bidmanova S, Dvorak P, Pavelka A, Chaloupkova R, Prokop Z, Damborsky J (2013) Haloalkane dehalogenases: biotechnological applications. Biotechnol J 8(1):32–45. https://doi.org/10.1002/biot.201100486

Larsen M, Guss A, Metcalf WW (2002) Genetic analysis of pigment biosynthesis in *Xanthobacter autotrophicus* Py2 using a new, highly efficient transposon mutagenesis system that is functional in a wide variety of bacteria. Arch Microbiol 178(3):193–201. https://doi.org/10.1007/s00203-002-0442-2

Lawrence J, Ochman H (1997) Amelioration of bacterial genomes: rates of change and exchange. J Mol Evol 44(4):383–397. https://doi.org/10.1007/PL00006158

Layton J, Wallace W, Corcoran C, Sayler GSAC (1992) Evidence for 4-chlorobenzoic acid dehalogenation mediated by plasmids related to pSS50. Appl Environ Microbiol 58(1):399–402

Li H, Durbin R (2010) Fast and accurate long-read alignment with burrows wheeler transform. Bioinformatics 26(5):589–595. https://doi.org/10.1093/bioinformatics/btp698

Li P-L, Hwang I, Miyagi H, True H, Farrand SK (1999) Essential components of the Ti plasmid *trb* system, a Type IV macromolecular transporter. J Bacteriol 181(16):5033–5041

Locher H, Leisinger T, Cook A (1991) 4-toluene sulfonate methyl-monooxygenase from Comamonas testosteroni T-2: purification and some properties of the oxygenase component. J Bacteriol 173(12):3741–3748. https://doi.org/10.1128/jb.173.12.3741-3748.1991

Lukashin M, Borodovsky A (1998) GeneMark.hmm: new solutions for gene finding. Nucleic Acids Res 26:1107–1115. https://doi.org/10.1093/nar/26.4.1107

Luo B, Xie Y, Li Z, Huang W, Yuan J, He G, Chen Y, Pan Q, Liu Y, Tang J, Wu G, Zhang H, Shi Y, Liu Y, Yu C, Wang B, Lu Y, Han C, Cheung DW, Yiu S-M, Peng S, Xiaoqian Z, Liu G, Liao X, Li Y, Yang H, Wang J, Lam T-W, Wang J (2012) SOAPdenovo2: an empirically improved memory-efficient short-read de novo assembler. Gigascience 1(1):18. https://doi.org/10.1186/2047-217X-1-18

Martinez B, Tomkins J, Wackett L, Wing R, Sadowsky M (2001) Complete nucleotide sequence and organization of the atrazine catabolic plasmid pADP-1 from *Pseudomonas* sp. strain ADP. J Bacteriol 183(19):5684–5677. https://doi.org/10.1128/JB.183.19.5684-5697.2001

Mulligan C, Fischer M, Thomas G (2011) Tripartite ATP-independent periplasmic (TRAP) transporters in bacteria and archaea. FEMS Microbiol Rev 35(1):68–86. https://doi.org/10.1111/j.1574-6976.2010.00236.x

Nagata Y, Endo R, Ito M, Ohtsubo Y, Tsuda M (2007) Aerobic degradation of lindane (γ-hexachlorocyclohexane) in bacteria and its biochemical and molecular basis. Appl Microbiol Biotechnol 76(4):741–752. https://doi.org/10.1007/s00253-007-1066-x

Nakatsu CH, Straus NA, Wyndham RC (1995) The nucleotide sequence of the Tn5271 3-chlorobenzoate 3, 4-dioxygenase genes (*cbaAB*) unites the class IA oxygenases in a single lineage. Microbiology 141:485–495. https://doi.org/10.1099/13500872-141-2-485

Overbeek R, Pusch GD, Olsen GJ, Davis JJ, Disz T, Edwards RA, Gerdes S, Parrello B, Shukla M (2014) The SEED and the rapid annotation of microbial genomes using subsystems technology (RAST). Nucleic Acids Res 42:D206–D214. https://doi.org/10.1093/nar/gkt1226

Petersen J, Brinkmann H, Pradella S (2009) Diversity and evolution of *repABC* type plasmids in *Rhodobacterales*. Environ Microbiol 11:2627–2638. https://doi.org/10.1111/j.1462-2920.2009.01987.x

Pieper D (2005) Aerobic degradation of polychlorinated biphenyls. Appl Microbiol Biotechnol 67(2):170–191. https://doi.org/10.1007/s00253-004-1810-4

Pieper D, Knackmuss H-J, Timmis KN (1993) Accumulation of 2-chloromuconate during metabolism of 3-chlorobenzoate by *Alcaligenes eutrophus* JMP134. Appl Microbiol Biotechnol 39(4–5):563–567. https://doi.org/10.1007/BF00205052

Prieto MA, Garcia JL (1994) Molecular characterization of 4-hydroxyphenylacetate 3-hydroxylase of *Escherichia coli*. A two-protein component enzyme. J Biol Chem 269(36):22823–22829

Reasoner DJ, Geldreich EE (1985) A new medium for the enumeration and subculture of bacteria from potable water. Appl Environ Microbiol 49(1):1–7

Ricker H, Qian H, Fulthorpe R (2013) Phylogeny and organization of recombinase in trio (RIT) elements. Plasmid 70(2):226–239. https://doi.org/10.1016/j.plasmid.2013.04.003

Riefert H, Rabenhorst J, Steinbüchel A (1997) Molecular characterization of genes of *Pseudomonas* sp. strain HR199 involved in bioconversion of vanillin to protocatechuate. J Bacteriol 179(8):2595–2607. https://doi.org/10.1128/jb.179.8.2595-2607.1997

Romanov V, Hausinger RP (1994) Pseudomonas aeruginosa 142 uses a three-component ortho-halobenzoate 1,2-dioxygenase for metabolism of 2,4-dichloro- and 2-chlorobenzoate. J Bacteriol 176(11):3368–3374. https://doi.org/10.1128/jb.176.11.3368-3374.1994

Rousseaux S, Soulas G, Hartmann A (2002) Plasmid localisation of atrazine-degrading genes in newly described *Chelatobacter* and *Arthrobacter* strains. FEMS Microbiol Ecol 41(1):69–75. https://doi.org/10.1111/j.1574-6941.2002.tb00967.x

Schuler L, Jouanneau Y, Ni Chadhain S, Meyer C, Pouli M, Zylstra G, Hols P, Agathos S (2009) Characterization of a ring-hydroxylating dioxygenase from phenanthrene-degrading *Sphingomonas* sp. strain LH128 able to oxidize *benz[a]anthracene*. Appl Microbiol Biotechnol 83(3):465–475. https://doi.org/10.1007/s00253-009-1858-2

Seyedsayamdost M, Case R, Kolter R, Clardy J (2011) The Jekyll-and-Hyde chemistry of *Phaeobacter gallaeciensis*. Nat Chem 3(4):331–335. https://doi.org/10.1038/nchem.1002

Sievers F, Higgins DG (2014) Clustal omega. Curr Protoc Bioinformatics 48(1):3.13.1–3.13.16. https://doi.org/10.1002/0471250953.bi0313s48

Simonsen A (2010) Physiological characterisation of bacteria degrading dichlobenil and linuron herbicides. 2010. PhD thesis university of Kopenhagen

Simonsen A, Holtze MS, Sørensen SR, Sørensen SJ, Aamand J (2006) Mineralisation of 2,6-dichlorobenzamide (BAM) in dichlobenil-exposed soils and isolation of a BAM-mineralising *Aminobacter* sp. Environ Pollut 144(1):289–295. https://doi.org/10.1016/j.envpol.2005.11.047

Simonsen A, Badawi N, Anskjær G, Albers C, Sørensen S, Sørensen J, Aamand J (2012) Intermediate accumulation of metabolites results in a bottleneck for mineralisation of the herbicide metabolite 2,6-dichlorobenzamide (BAM) by *Aminobacter* spp. Appl Microbiol Biotechnol 94(1):237–245. https://doi.org/10.1007/s00253-011-3591-x

Slater SC, Goldman BS, Goodner B, Setubal JC, Farrand SK, Nester EW, Burr TJ, Banta L, Dickerman AW, Paulsen I, Otten L, Suen G, Welch R, Almeida NF, Arnold F, Burton OT, Du Z, Ewing A, Godsy E, Heisel S, Houmiel KL, Jhaveri J, Lu J, Miller NM, Norton S, Chen Q, Phoolcharoen W, Ohlin V, Ondrusek D, Pride N, Stricklin SL, Sun J, Wheeler C, Wilson L, Zhu H, Wood DW (2009) Genome sequences of three *Agrobacterium* biovars help elucidate the evolution of multichromosome genomes in bacteria. J Bacteriol 191(8):2501–2511. https://doi.org/10.1128/JB.01779-08

Solyanikova IP, Emelyanova EV, Shumkova ES, Egorova DO, Korsakova ES, Plotnikova EG, Golovleva LA (2015) Peculiarities of the degradation of benzoate and its chloro- and hydroxy-substituted analogs by actinobacteria. Int Biodeterior Biodegrad 100:155–164. https://doi.org/10.1016/j.ibiod.2015.02.028

Sørensen SR, Holtze MS, Simonsen A, Aamand J (2007) Degradation and mineralization of nanomolar concentrations of the herbicide dichlobenil and its persistent metabolite 2,6-dichlorobenzamide by *Aminobacter* spp. isolated from dichlobenil-treated soils. Appl Environ Microbiol 73(2):399–406. https://doi.org/10.1128/aem.01498-06

Springael D, Ryngaert A, Merlin C, Toussaint A, Mergeay M (2001) Occurrence of Tn*4371*-related mobile elements and sequences in (chloro)biphenyl-degrading bacteria. Appl Environ Microbiol 67(1):42–50. https://doi.org/10.1128/AEM.67.1.42-50.2001

Starkenburg SR, Larimer FW, Stein LY, Klotz MG, Chain PSG, Sayavedra-Soto LA, Poret-Peterson AT, Gentry ME, Arp DJ, Ward B, Bottomley PJ (2008) Complete genome sequence of *Nitrobacter hamburgensis* X14 and comparative genomic analysis of species within the genus *Nitrobacter*. Appl Environ Microbiol 74(9):2852–2863. https://doi.org/10.1128/AEM.02311-07

Suzuki K, Ogawa N, Miyashita K (2001) Expression of 2-halobenzoate dioxygenase genes (*cbdSABC*) involved in the degradation of benzoate and 2-halobenzoate in *Burkholderia* sp. TH2. Gene 262(1–2):137–145. https://doi.org/10.1016/S0378-1119(00)00542-4

T'Syen J, Tassoni R, Hansen L, Sorensen SJ, Leroy B, Sekhar A, Wattiez R, De Mot R, Springael D (2015) Identification of the amidase BbdA that initiates biodegradation of the groundwater micropollutant 2,6-dichlorobenzamide (BAM) in *Aminobacter* sp. MSH1. Environ Sci Technol 49(19):11703–11713. https://doi.org/10.1021/acs.est.5b02309

Tabata S, Hooykaas P, Oka A (1989) Sequence determination and characterization of the replicator region in the tumor-inducing plasmid pTiB6S3. J Bacteriol 171(3):1665–1672. https://doi.org/10.1128/jb.171.3.1665-1672.1989

Tabata M, Endo R, Ito M, Ohtsubo Y, Kumar A, Tsuda M, Nagata Y (2011) The *lin* genes for γ-hexachlorocyclohexane degradation in *Sphingomonas* sp. MM-1 proved to be dispersed across multiple plasmids. Biosci Biotechnol Biochem 75(3):466–472. https://doi.org/10.1271/bbb.100652

Tabata M, Ohhata S, Nikawadori Y, Kishida K, Sato T, Kawasumi T, Kato H, Ohtsubo Y, Tsuda M, Nagata Y (2016) Comparison of the complete genome sequences of four γ-hexachlorocyclohexane-degrading bacterial strains: insights into the evolution of bacteria able to degrade a recalcitrant man-made pesticide. DNA Res 23(6):581–599. https://doi.org/10.1093/dnares/dsw041

Top EM, Springael D, Boon N (2002) Catabolic mobile genetic elements and their potential use in bioaugmentation of polluted soils and waters. FEMS Microbiol Ecol 42(2):199–208. https://doi.org/10.1111/j.1574-6941.2002.tb01009.x

Topp E, Zhu H, Nour SM, Houot S, Lewis M, Cuppels D (2000) Characterization of an atrazine-degrading *Pseudaminobacter* sp. isolated from Canadian and French agricultural soils. Appl Environ Microbiol 66(7):2773–2782. https://doi.org/10.1128/AEM.66.7.2773-2782.2000

Tralau T, Cook A, Ruff J (2001) Map of the IncP1β plasmid pTSA encoding the widespread genes (*tsa*) for p-toluenesulfonate degradation in *Comamonas testosteroni* T-2. Appl Environ Microbiol 67:1508–1516. https://doi.org/10.1128/AEM.67.4.1508-1516.2001

Tsoi TV, Plotnikova EG, Cole JR, Guerin WF, Bagdasarian M, Tiedje JM (1999) Cloning, expression, and nucleotide sequence of the *Pseudomonas aeruginosa* 142 *ohb* genes coding for oxygenolytic ortho dehalogenation of halobenzoates. Appl Environ Microbiol 65(5):2151–2162

Vrchotova B, Macková M, Macek T, Demnerová K (2013) Bioremediation of chlorobenzoic acids. In: Patil YB, Rao P (eds) Applied bioremediation - active and passive approaches. InTech, Rijeka, pp 3–32

Wick RR, Judd LM, Gorrie CL, Holt KE (2017) Unicycler: resolving bacterial genome assemblies from short and long sequencing reads. PLoS Comput Biol 13(6):e1005595. https://doi.org/10.1371/journal.pcbi.1005595

Young J, Crossman L, Johnston A, Thomson N, Ghazoui Z, Hull K, Wexler M, Curson A, Todd J, Poole P (2006) The genome of *Rhizobium leguminosarum* has recognizable core and accessory components. Genome Biol 7:R34. https://doi.org/10.1186/gb-2006-7-4-r34